The Undirected Team Orienteering Arc Routing Problem: Formulations, Valid Inequalities, and Exact Algorithms

Wenjin Yan[1], Elena Fernández[2], and Ivana Ljubić[1]

[1]ESSEC Business School, France , wenjin.yan@essec.edu, ivana.ljubic@essec.edu
[2]Universidad de Cádiz, Spain , elena.fernandez@uca.es

Abstract

We address the Undirected Team Orienteering Arc Routing Problem (UTOARP). In this problem, demand is placed at some edges of a given undirected graph and served demand edges produce a profit. Feasible routes must start and end at a given depot and there is a time limit constraint on the maximum duration of each route. The problem asks for a set of $|K|$ maximum profit routes. We exploit optimality conditions for this problem and propose two new undirected formulations with binary variables. We also introduce a logic-based Benders decomposition derived from these formulations and show how to strengthen the logic-based Benders cuts. Furthermore, we design several new families of valid inequalities, where some of them are derived from conflict graphs. We also develop a problem-specific GRASP-based heuristic to improve the performance of exact algorithms. Extensive computational tests are conducted to examine the performance of the proposed formulations, valid inequalities, and heuristics. Our findings highlight the pivotal role of logic-based Benders decomposition and conflict graphs in solving the UTOARP, marking their first application in the context of arc routing problems to the best of our knowledge. Moreover, these techniques hold promise for advancing solution approaches in broader arc routing contexts.

1 Introduction

Arc routing problems (ARPs) are a significant class of routing problems where service demand is associated with the links of a given network, as opposed to node routing problems where demand is located at nodes (vertices). Many real-world applications can be modeled as ARPs, including traditional ones such as snow plowing (Campbell et al., 2015), waste collection (Ghiani et al., 2015), and security patrolling (Huanfa Chen and Shawe-Taylor, 2018). More recently, with advancements in technology, ARPs have also emerged in applications such as meter reading (Corberán et al., 2021), road inspection and maintenance with drones (Campbell et al., 2018), and electric vehicle routing with wireless dynamic charging (Fernández et al., 2022). In these problems, a vehicle may traverse a link or a node multiple times in an optimal solution. This solution property adds complexity and difficulties to model construction and algorithm design, compared to node routing problems. To address these challenges, researchers have invested considerable effort in proposing strong formulations and efficient algorithms for various ARPs (e.g., Dror, 2000; Corberán and Laporte, 2015; Fernández et al., 2025).

Typically, ARPs assume that all service demand must be fulfilled, with the objective of minimizing travel costs. However, this approach is not always feasible or profitable in practice. In some cases, there may be a large amount of demand, but due to vehicle travel time or capacity constraints, it is not possible to serve all of it. In other cases, it may not be profitable to serve links with low profit and high traversal cost. Therefore, decision-makers may prefer to only serve a subset of the demand, including the most profitable links. The subclass of ARPs that addresses this type of problems is known as *ARPs with profits* (see, e.g., Archetti and Speranza, 2015), and includes both single- and multiple-vehicle variants. This paper focuses on one such multiple-vehicle variant: the Team Orienteering Arc Routing Problem (TOARP). In the TOARP, demand

links are associated with profits, and there is a fleet of vehicles, each of them with a maximum travel time limit. The problem is to select a subset of demand links to be served and a route for each vehicle in order to maximize total profits while adhering to the travel time limit. The travel time limit is relevant in many practical applications, such as the maximum travel distance for winter service vehicles or the working time limit for police officers conducting patrols. The TOARP can be viewed as the arc routing counterpart of the Team Orienteering Node (Vehicle) Routing Problem (TOVRP, see, e.g., Gunawan et al., 2016).

1.1 Contributions

The contributions of this paper can be summarized as follows:

- Like other routing problems in the literature, the TOARP can be investigated on different types of graphs: directed, undirected, mixed, or windy. Each type of graph possesses distinct properties, so tailored models and algorithms are needed for each specific problem. In this paper, we study the TOARP on undirected graphs (UTOARP). Making use of an optimality condition that only applies to the undirected version of the problem, we propose two new formulations with binary variables defined on different spaces. The first model is a disaggregated formulation, with service variables being defined per vehicle and per profitable edge. The other one is a semi-aggregrated formulation, with a single binary service variable being defined for each profitable edge. To the best of our knowledge, these are the first ILP formulations for the problem defined in the space of binary variables associated with edges.

- Given the multiple-vehicle structure of the UTOARP, decomposition methods such as Dantzig-Wolfe decomposition (DWD) or Benders decomposition (BD) are natural choices for solving the problem. However, existing studies on multiple-vehicle ARPs have primarily focused on DWD (see, e.g., Bode and Irnich, 2012; Bartolini et al., 2013). BD has received little attention in the context of ARPs, largely because classical BD applies only when the subproblem is a linear program, whereas most ARP formulations involve only integer variables. In this paper, we address this challenge by applying a more general BD approach, namely Logic-Based Benders Decomposition (LBBD, Hooker, 2024), which constitutes one of our core contributions. To the best of our knowledge, this is the first time an LBBD approach is applied in the context of arc routing.

- We introduce several new families of valid inequalities based on the optimality condition of the undirected problem, including *inaccessible first and second traversal* inequalities, *clique* inequalities, and *independent set* inequalities. Notably, *clique* and *independent set* inequalities are derived from *conflict graphs*, which, as far as we know, have not been leveraged in ARPs before. We also present *symmetry breaking* constraints and *strengthened logic-based Benders* cuts. We customize these inequalities for each of the three proposed formulations.

- We propose efficient (heuristic and exact) procedures for the separation and generation of valid inequalities. We also show how to use these procedures to repair infeasible solutions and refine feasible ones. Additionally, we use a GRASP-based heuristic to find an initial incumbent solution.

- We conduct extensive computational tests to examine the performance of the three proposed formulations, valid inequalities, and heuristics. Our new formulations are compared against a compact, load-based formulation, which is used as a benchmark. The results show that the performance of the formulations improves significantly with the addition of the inequalities and heuristics. Moreover, the logic-based Benders reformulation demonstrates superiority over the other formulations. Additionally, we perform sensitivity analysis with respect to the travel time limit and the number of vehicles, further confirming the computational advantages of the logic-based Benders reformulation in different settings.

- Our study demonstrates that the use of LBBD and conflict graphs unveils significant potential for future research in ARPs. Specifically, for multiple-vehicle ARPs, LBBD allows for a natural problem decomposition into a series of simpler arc routing subproblems, each corresponding to a single vehicle. After decomposition, the subproblems are significantly easier to solve in practice due to their reduced instance size. On the other hand, conflict graphs effectively capture key structural properties

Problem	Reference	Graph	Vehicle $T_{\max}$	Vehicle C	Multi-visits	Objective	Model	Algorithm
DTOARP	Archetti et al. (2014)	D	✓			max profits	Arc-based	B&C
	Archetti et al. (2015)	D	✓			max profits		Heuristic
	Riera-Ledesma and Salazar-González (2017)	D	✓			max profits	Route-based	B&C&P
MTOARP	Benavent et al. (2015)	M	✓	✓		max profits	Load-based	B&B
PATP	Feillet et al. (2005)	D	✓		✓	max profits - time	Route-based	B&P
	Euchi and Chabchoub (2011)	D	✓		✓	max profits - time		Heuristics
UCARPP	Archetti et al. (2010)	U	✓	✓		max profits	Route-based	B&P
	Zachariadis and Kiranoudis (2011)	U	✓	✓		(1) max profits (2) min time		Heuristic
UTOARP	This work	U	✓			max profits	Edge-based	Benders

Note: For the graph, U, D, and M denote undirected, directed, and mixed graphs, respectively.

Table 1: Summary of Related Literature

of undirected ARPs. These graphs encode rich information about problem constraints and interactions, providing a strong foundation for deriving valid inequalities. By leveraging different conflict graph structures, the inequalities derived from conflict graphs can be used to strengthen formulations and significantly improve computational efficiency. Our findings suggest that these techniques offer promising directions for enhancing the solution methods in ARPs.

1.2 Literature Review

In this section, we review the literature on multiple-vehicle ARPs with profits where vehicles have a time limit. A summary of the related work is presented in Table 1. For each problem (column Problem), the table lists the references (column Reference) and key characteristics, including the type of graph the problem is defined on (column Graph), the constraints on vehicles such as travel time limit (column $T_{\max}$) and capacity limit (column C), whether edge profits can be collected multiple times (column Multi-visits), the objective (column Objective), the type of variables used in the model (column Model), and the algorithms used for solution procedures (column Algorithm). For a broader overview of ARPs with profits, we refer interested readers to the relevant book chapter by Archetti and Speranza (2015) and the survey by Corberán and Laporte (2015).

Existing studies on the TOARP and related problems primarily focus on directed graphs (Archetti et al., 2014, 2015; Riera-Ledesma and Salazar-González, 2017) and mixed graphs (Benavent et al., 2015). In addition to a set of edges with profits (*profitable* edges) that are optional to traverse, these studies also consider another set of edges that must be traversed (*required* edges). Note that one can ensure that all *required* edges are served by assigning them a sufficiently large profit.

For the directed TOARP, Archetti et al. (2014) propose a two-index formulation with an exponential number of constraints and study a relaxation of its polyhedron. They introduce several families of valid inequalities, namely path-bridge, K-C, and max-length, and incorporate them into a Branch-and-Cut (B&C) algorithm. Archetti et al. (2015) propose a matheuristic for the same problem, which includes a Tabu Search (TS) and a diversification step. Riera-Ledesma and Salazar-González (2017) use a graph transformation to represent the demand on nodes instead of arcs. For the problem on the transformed graph, they propose a three-index formulation using binary variables only. Moreover, they obtain two set partitioning formulations based on the DWD: one contains elementary routes only and the other allows non-elementary routes. For each set partitioning formulation they design two exact algorithms, a Branch-and-Price (B&P) and a Branch-and-Cut-and-Price (B&C&P).

For the mixed TOARP, Benavent et al. (2015) consider two variants: (1) the Team Orienteering Mixed Capacitated Arc Routing Problem, where each edge is associated with a demand and vehicles have capacity limits; and (2) the Team Orienteering Mixed Uncapaciated Arc Routing Problem, where edges have no associated demand and vehicles are uncapacitated. They propose a load-based compact formulation for each variant and solve them with a Branch-and-Bound (B&B) algorithm.

Compared to the variants on directed and mixed graphs, the undirected problem has a unique property: there exists an optimal solution where each edge is traversed at most twice by each vehicle (Christofides, 1981; Corberán and Sanchis, 1994). This property not only allows us to develop formulations using binary decision variables but also helps in developing valid inequalities to strengthen these formulations. In contrast, this property does not generally hold for the other two variants, which motivates our focus on the undirected problem.

Other related problems include the Profitable Arc Tour Problem (PATP, Feillet et al., 2005; Euchi and Chabchoub, 2011) and the Capacitated Arc Routing Problem with Profits (CARPP, Archetti et al., 2010; Zachariadis and Kiranoudis, 2011).

The PATP, introduced by Feillet et al. (2005), is defined on a complete directed graph and differs from the TOARP in several ways: the profits of each arc can be collected multiple times, the objective is to minimize the difference between total profits and travel time, vehicles can start and end at any node of the graph, and the number of vehicles used is not fixed. A B&P algorithm is designed to solve this problem. In the follow-up work of Euchi and Chabchoub (2011), two meta-heuristics are introduced, which combine the Adaptive Memory Procedure (AMP) with the TS and Variable Neighborhood Search (VNS), respectively.

The CARPP considers the demand of each edge and assumes capacitated vehicles, thus adding a capacity constraint for each vehicle. Archetti et al. (2010) present a set packing formulation for this problem in an undirected graph and propose a B&P algorithm and three heuristics, namely one VNS and two TS. Zachariadis and Kiranoudis (2011) introduce a hierarchical objective function, prioritizing the maximization of total profits collected and secondarily minimizing travel time. Then they develop a Local Search (LS) heuristic for this problem.

The undirected CARPP can be seen as a generalization of our setting, with additional capacity constraints. However, many real-world applications (e.g., snow plowing, security patrolling, road maintenance) involve only time limit constraints, which is why we do not consider capacity constraints. This is also consistent with the majority of the literature on directed and mixed TOARP mentioned above, as well as the classical TOVRP (see, e.g., Gunawan et al., 2016). Furthermore, from modeling perspective, existing works do not fully exploit the properties of undirected graphs, which we show have significant untapped potential for further exploration.

Regarding solution methods, to the best our knowledge, there is no work that uses BD for ARPs.

1.3 Organization of the Paper

The rest of this paper is organized as follows. In Section 2, we formally define the UTOARP and discuss the optimality condition. Then, we develop two new undirected formulations in Section 3. Based on these new formulations, we show how to decompose the problem using LBBD in Section 4. In Section 5, we introduce several new families of valid inequalities and adapt them for each formulation. In Section 6, we design several heuristics and detail the separation and generation procedures of valid inequalities. Computational results are presented and analyzed in Section 7, and conclusions are highlighted in Section 8. In the appendix, we present more details on valid inequalities, heuristics, computational results, as well as a compact load-based formulation, which is used as a benchmark against the new proposed models.

2 Problem Definition and Solution Properties

In this section, we formally define the UTOARP and introduce the notation in Section 2.1. We then present the optimality condition of this problem in Section 2.2.

2.1 Problem Definition and Notation

Consider an undirected graph $G = (V, E)$, where V is the set of vertices with 0 as the depot, and E is the set of edges. Each edge $e \in E$ is associated with a travel time $t_e > 0$. Let $E_P \subseteq E$ be a given subset of edges, referred to as *profitable* edges, each of them, associated with a positive profit r_e. The profit r_e is collected if profitable edge $e \in E_P$ is served. The remaining set of edges, denoted as $E_{NP} = E \setminus E_P$, is the set of *non-profitable* edges. There is a fleet of vehicles indexed by the set K, each of them having a time limit $T_{\max}$ for the maximum duration of its corresponding route. Profitable edges $e \in E_P$ can be traversed by all

vehicles, but can be served by at most one of the vehicles so their profits can be collected at most once. A tour for a given vehicle corresponds to a route which begins and ends at the depot, and a feasible tour is one whose total duration does not exceed the specified travel time limit. The UTOARP is to find a set of at most $|K|$ feasible tours of total maximum profit.

Without loss of generality we do not explicitly consider *required edges*, i.e., demand edges that must be necessarily served. They can be considered as profitable edges by assigning them a very large profit to ensure they are served by some vehicle $k \in K$.

The *undirected formulations* we will develop work on the undirected graph G using the following notation. Given a subset of vertices $S \subset V$, let $E(S) = \{e = ij \in E \mid i, j \in S\}$ be the set of edges with both end-vertices in S and $\delta(S) = \{e = ij \in E \mid i \in S, j \in V \setminus S\}$ be the cut-set of S. For singleton sets, $\delta(\{i\})$ is simplified as $\delta(i)$. For $S \subset V$, define $E_P(S) = E(S) \cap E_P$ as the set of profitable edges with both end-vertices in S and $\delta_P(S) = \delta(S) \cap E_P$ as the set of profitable edges in the cut-set of S. Similarly, for non-profitable edges, define $E_{NP}(S) = E(S) \cap E_{NP}$ and $\delta_{NP}(S) = \delta(S) \cap E_{NP}$. For simplicity, the summation of a vector $y \in \mathbb{R}^{|E|}$ over a set $F \subset E$ is written as $y(F) = \sum_{e \in F} y_e$.

A problem closely related to the UTOARP with a single vehicle is the Undirected Rural Postman Problem (URPP, see, e.g., Ghiani and Laporte, 2015). Consider again the undirected graph $G = (V, E)$, let $E_R \subseteq E$ denote a subset of *required* edges that must be served. The objective of the URPP is to find a tour that visits all *required* edges $e \in E_R$ while minimizing travel time. For each vehicle's tour in the UTOARP, it is evident that an optimal solution exists where the vehicle follows the tour of a URPP. Specifically, once the set of profitable edges is selected for a vehicle in the UTOARP, the feasibility of these edges with respect to the time limit can be verified by finding a tour that minimizes travel time while covering all the selected edges (i.e., required edges), which is exactly the objective of the URPP.

2.2 Optimality Condition

In optimal solutions to the UTOARP, each edge can be traversed multiple times by a vehicle. For each traversal of an edge, the vehicle can either *serve* the edge and thus collect its associated profit, or simply *deadhead* it (traverse it without serving it).

For the URPP, there is a well-known optimality condition:

Theorem 2.1. *(Christofides, 1981; Corberán and Sanchis, 1994) Given an instance of the URPP on an undirected graph, there exists an optimal solution where each edge is traversed at most twice.*

Given the connection between the URPP and a single tour of the UTOARP mentioned above, we can extend this optimality condition of the URPP to the UTOARP:

Corollary 2.2. *Given an instance of the UTOARP on an undirected graph, there exists an optimal solution where each edge is traversed at most twice by each vehicle.*

This allows us to derive formulations using binary variables instead of integer variables for edge deadheads or traversals of each vehicle, which are presented in the following sections.

3 New Undirected Formulations

In this section, we present two novel formulations developed on the original undirected graph G utilizing binary variables only. The main difference between the two formulations is the way in which served edges are modeled. The first one identifies explicitly the vehicle that serves each edge. Instead, the second one identifies implicitly served edges by noting that any profitable edge that is traversed in the tour of some vehicle will be served. Specifically, the first formulation employs disaggregated service variables, one variable per profitable edge and vehicle (see Section 3.1), whereas the second formulation aggregates the service variables over all vehicles (see Section 3.2).

3.1 Disaggregated Formulation with Traversal Variables

We first introduce a formulation using disaggregated service and traversal variables. Given the optimality condition, we can use two sets of binary variables for edge traversals: $s_e^k \in \{0, 1\}$ is 1 if the profitable edge

$e \in E_P$ is served by the vehicle $k \in K$ and 0 otherwise, $y_e^k \in \{0,1\}$ is 1 if the edge $e \in E$ is traversed for the first time by the vehicle $k \in K$ and 0 otherwise, and $Y_e^k \in \{0,1\}$ is 1 if the edge $e \in E$ is traversed for the second time by the vehicle $k \in K$ and 0 otherwise.

We will assume that, if a profitable edge is traversed twice by a vehicle and the service is included, the first traversal corresponds to the service, and the second one to the deadhead. Note that this can be done without loss of generality. The formulation (referred to as U-DT) is as follows:

$$\max_{\substack{\mathbf{s}\in\{0,1\}^{|E_P||K|} \\ \mathbf{y},\mathbf{Y}\in\{0,1\}^{|E||K|}}} \sum_{k\in K}\sum_{e\in E_P} r_e s_e^k \tag{1a}$$

$$\text{s.t.} \sum_{k\in K} s_e^k \le 1, \qquad \forall e \in E_P, \tag{1b}$$

$$\sum_{e\in E} t_e(y_e^k + Y_e^k) \le T_{\max}, \qquad \forall k \in K, \tag{1c}$$

$$(y^k - Y^k)(\delta(S)\setminus F) + Y^k(F) \ge y^k(F) - |F| + 1, \qquad \forall S \subset V,\ F \subseteq \delta(S),\ |F| \text{odd},\ k \in K, \tag{1d}$$

$$(y^k + Y^k)(\delta(S)) \ge 2y_e^k, \qquad \forall S \subseteq V \setminus \{0\},\ e \in E_P(S),\ k \in K, \tag{1e}$$

$$Y_e^k \le y_e^k, \qquad \forall e \in E,\ k \in K, \tag{1f}$$

$$s_e^k \le y_e^k, \qquad \forall e \in E_P,\ k \in K. \tag{1g}$$

The objective function (1a) is to maximize the total profits collected. Constraints (1b) ensure each profitable edge can be served at most once over all vehicles. Constraints (1c) ensure the travel time limit $T_{\max}$ is respected by each vehicle. Co-circuit constraints (1d) (Barahona and Grötschel, 1986) ensure the number of traversed edges incident to each vertex is even in the tour of each vehicle. Specifically, when the edges in F are traversed for the first time, the right-hand-side of the constraint equals 1. Since $|F|$ is odd, the cut-set of S has to be traversed at least one more time to resolve the oddity. This additional traversal arises either from a single traversal of some edge in $\delta(S) \setminus F$, or a second traversal of some edge in F. If this constraint is imposed for each vertex set $S \subset V$, then each vertex in the tour has an even degree with respect to the traversed edges. This type of constraints can only be used in combination with binary variables to impose parity in undirected graphs. Constraints (1e) enforce the connectivity of the tour for each vehicle. Constraints (1f) require that an edge cannot be traversed for the second time without being traversed for the first time. Constraints (1g) state that if a profitable edge is served by a given vehicle, then it must be traversed by that vehicle. With these constraints, we also impose that if a profitable edge is served and deadheaded once by a vehicle, then its service takes place in its first traversal.

This formulation has $(|E_P| + 2|E|)|K|$ binary variables. However, it includes an exponential number of constraints due to (1d) and (1e).

3.2 Semi-Aggregated Formulation with Traversal Variables

In this formulation, for each profitable edge, we aggregate the service variables s_e^k over all vehicles $k \in K$ since we are ultimately interested in finding the subset of profitable edges that will be served.

- $z_e \in \{0,1\}$ takes 1 if profitable edge $e \in E_P$ is served and 0 otherwise.

With this aggregation, we can reduce the number of service decision variables, using again traversal variables to describe the tour of each vehicle. The formulation (referred to as U-ST) is:

$$\max_{\substack{\mathbf{z}\in\{0,1\}^{|E_P|} \\ \mathbf{y},\mathbf{Y}\in\{0,1\}^{|E||K|}}} \sum_{e\in E_P} r_e z_e \tag{2a}$$

$$\text{s.t. (1c)} - \text{(1f)},$$

$$\sum_{k\in K} y_e^k \ge z_e, \qquad \forall e \in E_P. \tag{2b}$$

The objective function maximizes the total profits, and $\sum_{k\in K} y_e^k \ge z_e$ states that if a profitable edge e is served, it must be traversed by at least one vehicle.

Now the number of binary variables is reduced to $|E_P| + 2|E||K|$. This way potentially reduces the execution time of the new model. However, this model still includes an exponential number of constraints (1d) and (1e). Moreover, once an optimal solution is obtained, in a post-processing phase, one can assign each served edge to the vehicle with the smallest index that traverses it.

4 Logic-Based Benders Reformulation

As mentioned, the two new undirected formulations contain an exponential number of connectivity and co-circuit constraints required to guarantee the feasibility of each tour. However, the variables involved in these constraints are not directly related to our objective: finding the most profitable combination of edges to serve. Following this insight and recognizing the problem's multiple-vehicle structure, we decompose the problem into two stages: in the first stage, the set of profitable edges is partitioned and assigned to the available vehicles; in the second stage, for each vehicle and the given set of assigned profitable edges, the optimal URPP solution determines the tour that minimizes its travel time. If, for a given vehicle, the travel time exceeds $T_{\max}$, the given assignment of profitable edges is infeasible and must be discarded. This rationale not only highlights the complexity of the UTOARP but also suggests the use of BD (see Rahmaniani et al., 2017; Clautiaux and Ljubić, 2024). Indeed, once the edges to serve by each vehicle are fixed, the problem decomposes into $|K|$ simpler URPPs, which aligns with the spirit of BD. However, classical BD applies only when the subproblem is a linear program, whereas our formulations involve only binary decision variables and the subproblems are NP-hard, which is why we opt for LBBD approach.

LBBD (Hooker, 2024) is a more general BD approach that allows the subproblems with integer variables. Unlike traditional BD, it does not involve a standard procedure for deriving Benders cuts; instead, cuts are generated based on the specific problem structure, referred to as Logic-Based Benders cuts (LBBCs). To employ LBBD for the UTOARP, we retain the service variables in the master problem and project out the traversal variables into the subproblems. Then the original UTOARP is decomposed into a relaxed master problem and a series of *feasibility* subproblems. Although these subproblems are NP-hard, they are significantly simpler than the original UTOARP. Moreover, as feasibility problems, they do not necessarily need to be solved to optimality, further underscoring the practicality and potential efficiency of this approach.

In the following, we present the relaxed master problem in Section 4.1 and the subproblem in Section 4.2. Then we introduce the Benders cuts in Section 4.3 and show how to strengthen them in Section 4.4. The Benders reformulation is shown in Section 4.5.

Throughout we will say that a given subset of profitable edges, $H \subseteq E_P$, is a *Feasible Profitable Subset* (FPS) if it is possible to serve all its edges in a feasible URPP tour without violating the time limit constraint. If, on the contrary, this is not possible we will say that $H \subseteq E_P$ is an *infeasible Profitable Subset* (IPS). Moreover, for a given vector of service variables $\mathbf{s}$, we use the notation $P(\mathbf{s}^k) = \{e \in E_P \mid s_e^k = 1,\ e \in E_P\}$ to denote the subset of profitable edges served by vehicle $k \in K$. Therefore, $\mathbf{s}$ induces a feasible solution to the UTOARP if and only if $P(\mathbf{s}^k)$ is an FPS for all $k \in K$.

4.1 Relaxed Master Problem

Projecting out the traversal variables in U-DT, we obtain the relaxed master problem (RMP):

$$\max_{\mathbf{s}\in\{0,1\}^{|E_P||K|}} \sum_{k\in K}\sum_{e\in E_P} r_e s_e^k \tag{3a}$$

$$\text{s.t.} \sum_{k\in K} s_e^k \leq 1, \qquad \forall e \in E_P, \tag{3b}$$

where we only retain the service constraints (3b). Violated Benders cuts are then detected by solving the Benders subproblems described below. They are dynamically inserted into the existing RMP, until optimality is proved (Hooker, 2024).

4.2 Subproblems

Given a solution $\bar{\mathbf{s}}$ from the current RMP, we need to check whether $P(\bar{\mathbf{s}}^k)$ is an FPS for all $k \in K$. Specifically, for a vehicle k and its corresponding $P(\bar{\mathbf{s}}^k)$, we construct an auxillary undirected graph $G^k =$

(V, E), where the edges in $P(\bar{\mathbf{s}}^k)$ are considered as *required* edges that must be served. We then check whether the minimum travel time to serve these edges (denoted as $T^*(P(\bar{\mathbf{s}}^k))$) exceeds the time limit $T_{\max}$. Finding $T^*(P(\bar{\mathbf{s}}^k))$ is equivalent to solving an instance of the URPP. Therefore, the Subproblems (SPs), originally *feasibility problems*, can be reformulated as a series of URPPs, one for each vehicle $k \in K$. For any vehicle $k \in K$, $P(\bar{\mathbf{s}}^k)$ is an FPS if and only if $T^*(P(\bar{\mathbf{s}}^k)) \leq T_{\max}$. Otherwise, $P(\bar{\mathbf{s}}^k)$ is an IPS, and a Benders cut should be added to cut off this solution, which will be detailed in the following sections.

Although the URPP remains NP-hard theoretically (Orloff, 1976), it can be solved quickly in practice, particularly in our case, where the instance size of the URPP is significantly reduced after decomposition. Moreover, we only need to know whether there exists a URPP solution whose travel time does not exceed $T_{\max}$. The detailed implementation procedure is presented in Section 6.1.

4.3 Logic-Based Benders Feasibility Cuts

Since the SPs are *feasibility problems*, only *feasibility cuts* are needed to determine the feasible domain for the $\mathbf{s}$ variables. For a given k and IPS $H \subseteq E_P$ for this vehicle, one could impose standard no-good cuts to cut off this infeasible solution:

$$s^k(E_P \setminus H) + (\mathbf{1} - s^k)(H) \geq 1, \qquad \forall k \in K, \forall H \subseteq E_P \text{ IPS}. \tag{4}$$

These cuts ensure that any new solution must differ from the current infeasible solution by either serving at least one edge from the unserved set $E_P \setminus H$ or not serving at least one edge from the served set H. These cuts can be further strengthened by noticing that $T^*(H)$ is a *monotone* function, meaning that if we insert one or more elements to an IPS H, the set remains infeasible. Therefore, we can add the following Benders feasibility cuts instead, which are sometimes called *monotone nogood* cuts (see, Hooker, 2024):

$$s^k(H) \leq |H| - 1, \qquad \forall k \in K, \forall H \subseteq E_P \text{ IPS}. \tag{5}$$

Using Benders feasibility cuts (5), one can eliminate all IPSs from the RMP, thus ensuring that the travel time limit constraints (1c) are respected.

4.4 Strengthened Logic-Based Benders Cuts

A given IPS $H \subseteq E_P$ is *irreducible* if it contains no IPS as a strict subset. Given an IPS $H \subseteq E_P$, one can strengthen the cut (5) by identifying an irreducible subset $H' \subseteq H$. Then the *Strengthened Logic-Based Benders cuts* (SLBBCs) can be written as:

$$s^k(H') \leq |H'| - 1, \qquad \forall k \in K, \forall H' \subseteq E_P \text{ irreducible IPS}. \tag{6}$$

It is in general NP-hard to find a minimum cardinality irreducible IPS (Gleeson and Ryan, 1990; Amaldi et al., 2003). We will show how to heuristically separate these cuts in Section 6.2.1. Our heuristic searches for a smaller subset of a given IPS (not necessarily irreducible) that may possibly induce a stronger Benders cut. In this context, we introduce the notion of *reduced IPS* (RIPS) as follows: given an IPS $H \subseteq E_P$, a subset $H' \subset E_P$ is called RIPS, if it is strictly contained in H and is an IPS. The goal of heuristics will be to take an IPS H and to find a RIPS H', which is not guaranteed to be minimal nor irreducible, but which will generate a stronger cut than the one imposed by the set H.

4.5 Benders Reformulation

Since the feasibility cuts (6) guarantee the travel time limit constraints (1c), and any feasible solution to the URPP satisfies (1d)-(1g) for each vehicle $k \in K$, the following logic-based Benders reformulation (referred to as LBBD) is valid for the UTOARP:

$$\max_{\mathbf{s} \in \{0,1\}^{|E_P||K|}} \sum_{k \in K} \sum_{e \in E_P} r_e s_e^k \tag{7a}$$

$$\text{s.t. } s^k(H) \leq |H| - 1, \qquad \forall k \in K, \forall H \subseteq E_P \text{ irreducible IPS}, \tag{7b}$$

$$\sum_{k \in K} s_e^k \leq 1, \qquad \forall e \in E_P. \tag{7c}$$

Since LBBD is an integer linear programming formulation with an exponential number of constraints, we solve it by employing a Branch-and-Benders-cut framework. In this way, the integer solutions found in the branching process will be sent to the subproblem to check the feasibility and thus the Benders feasibility cuts (7b) will be dynamically separated.

5 Valid Inequalities

In this section, we introduce several families of new valid inequalities for formulations U-DT, U-ST and LBBD to enhance the performance of the exact algorithms. We first present inequalities that forbid the inaccessible first and second traversals in Section 5.1. Based on them, we build conflict graphs and derive clique and independent set inequalities in Section 5.2. Then, we show symmetry breaking constraints in Section 5.3. Lastly, we adapt SLBBCs in Section 5.4. Each type of inequality is tailored to the specific formulation it addresses.

5.1 Inaccessible Traversals

In this section we present conditions that, given the travel time limit $T_{\max}$, identify and exclude edges that cannot be traversed by vehicles in feasible tours. Such constraints are prevalent in orienteering problems (Keller, 1989; Leifer and Rosenwein, 1994; El-Hajj et al., 2016), and here we extend them to the UTOARP.

5.1.1 Inaccessible First Traversals

Let d_{ij} denote the minimum travel time from vertex $i \in V$ to $j \in V$ (i.e. the length of the shortest path from i to j with respect to travel time), and l_{ie}^1 denote the minimum travel time of any tour starting and ending at vertex $i \in V$ that traverses $e = uv \in E$ once, (i.e., $l_{ie}^1 = d_{iu} + t_e + d_{vi}$).

Definition 1. *An edge $e \in E$ is* inaccessible for the first traversal *if $l_{0e}^1 > T_{\max}$.*

That is, edge $e \in E$ is inaccessible for the first traversal if it cannot be traversed even once in any feasible tour. An illustration of the minimum travel time l_{0e}^1 is provided in Appendix A.1.

Let $E^1 = \{e \in E \mid l_{0e}^1 > T_{\max}, \forall e \in E\}$ represent the set of edges inaccessible for the first traversal. We further categorize such edges into profitable and non-profitable ones, i.e., $E_P^1 = E^1 \cap E_P$ and $E_{NP}^1 = E^1 \cap E_{NP}$, respectively. Feasibility conditions can be derived for each formulation.

For U-DT, we can forbid service and traversals of inaccessible profitable edges and traversals of inaccessible non-profitable edges as follows:

$$\sum_{k \in K} (s^k + y^k + Y^k)(E_P^1) = 0, \tag{8a}$$

$$\sum_{k \in K} (y^k + Y^k)(E_{NP}^1) = 0. \tag{8b}$$

For U-ST, the constraints are the same as (8b) in U-DT for non-profitable edges E_{NP}^1. For profitable edges E_P^1, the disaggregated service variables $\mathbf{s}$ are replaced with aggregated ones $\mathbf{z}$:

$$(z + \sum_{k \in K} (y^k + Y^k))(E_P^1) = 0. \tag{9}$$

For LBBD, we can only forbid the service for the inaccessible profitable edges E_P^1:

$$\sum_{k \in K} s^k(E_P^1) = 0. \tag{10}$$

Note that the constraints developed above can be either directly imposed in the formulations, or incorporated in a preprocessing procedure that removes these edges from G.

5.1.2 Inaccessible Second Traversals

Similarly to inaccessible first traversals, an edge is inaccessible for *the second traversal* if the minimum travel time to traverse it twice in any tour exceeds $T_{\max}$. Let l^2_{ie} denote this minimum travel time of any tour starting and ending at $i \in V$ that traverses the edge $e = uv \in E$ twice, i.e., $l^2_{ie} = \min\{d_{iu} + 2t_e + d_{ui},\ d_{iv} + 2t_e + d_{vi}\}$. Then we define:

Definition 2. *An edge $e \in E$ is inaccessible for the second traversal if $l^2_{0e} > T_{\max}$.*

The possible tours contributing l^2_{0e} are visualized in Appendix A.1.

Let $E^2 = \{e \in E \mid l^2_{0e} > T_{\max}, \forall e \in E\}$, and we categorize profitable and non-profitable edges as $E^2_P = E^2 \cap E_P$ and $E^2_{NP} = E^2 \cap E_{NP}$, respectively. Feasibility conditions can be customized for the different formulations as follows.

For U-DT and U-ST, second traversals are not permitted for $e \in E^2$.

$$\sum_{k \in K} Y^k(E^2) = 0. \tag{11}$$

For LBBD, these constraints cannot be expressed solely in terms of service variables. However, they can be incorporated into the subproblem to enhance computational efficiency of the Benders cut separation procedure.

5.2 Inequalities from Conflict Graphs

Conflict (intersection or incompatibility) graphs represent the conflict relationships between elements of a given optimization problem. In the UTOARP, for example, two *edges* are in conflict if they can not be traversed in the same feasible tour, or two *binary variables* are in conflict if they cannot both take the value one simultaneously. By identifying these conflict relationships, one can construct conflict graphs, where the vertex set consists of the elements themselves (i.e., edges or binary variables), and the edge set is defined based on the conflicts between pairs of elements.

Specifically, in the UTOARP, we define the edges in conflict as follows:

Definition 3. *Two distinct edges $e, e' \in E$ are in conflict if $L_{\min}(e, e') > T_{\max}$.*

where $L_{\min}(e, e')$ is the minimum travel time of any tour that traverses two given distinct edges $e = ij, e' = i'j' \in E, e \neq e'$ exactly once. Formally, $L_{\min}(e, e') = \min\{d_{0i} + t_e + d_{ji'} + t_{e'} + d_{j'0},\ d_{0i} + t_e + d_{jj'} + t_{e'} + d_{i'0},\ d_{0j} + t_e + d_{ii'} + t_{e'} + d_{j'0},\ d_{0j} + t_e + d_{ij'} + t_{e'} + d_{i'0}\}$, where we recall, d_{ij} denotes the minimum travel time from vertex i to vertex j. In Appendix A.1, the possible tours contributing $L_{\min}(e, e')$ are demonstrated.

To illustrate conflict graphs, we use the following example:

Example 5.1. *Consider an instance of the UTOARP with seven edges $E = \{e_1, ..., e_7\}$. As shown in Figure 1a, the profitable edges (depicted as blue vertices) are $E_P = \{e_1, e_2, e_5, e_6, e_7\}$ and the non-profitable edges (depicted as white vertices) are $E_{NP} = \{e_3, e_4\}$. Each pair of edges in conflict is represented by a blue line connecting their corresponding vertices. We suppose that no edge is inaccessible for the first traversal, i.e., $E^1 = \emptyset$, but the inaccessible set for the second traversal is $E^2 = \{e_2, e_4\}$. Thus, $E^2_P = \{e_2\}$ and $E^2_{NP} = \{e_4\}$.*

From conflict graphs, one can derive clique (see, e.g., Padberg, 1973) and independent set (IS) inequalities (El-Hajj et al., 2016). Specifically, clique inequalities identify complete subgraphs (i.e., cliques) within the conflict graph and constrain the selection of elements in a clique to at most one. Conversely, IS inequalities focus on individual elements. For an element in the conflict graph, by constructing a subgraph of the conflict graph induced by the element and its neighbors, these inequalities restrict the selection of its neighbors based on the size of the maximum independent set in the subgraph.

In this section, we present formulation-specific conflict graphs and derive inequalities from these graphs. Specifically, we construct the *edge conflict graph* and derive *clique inequalities* in Section 5.2.1. Then we build the *variable conflict graph* and propose *IS inequalities* in Section 5.2.2.

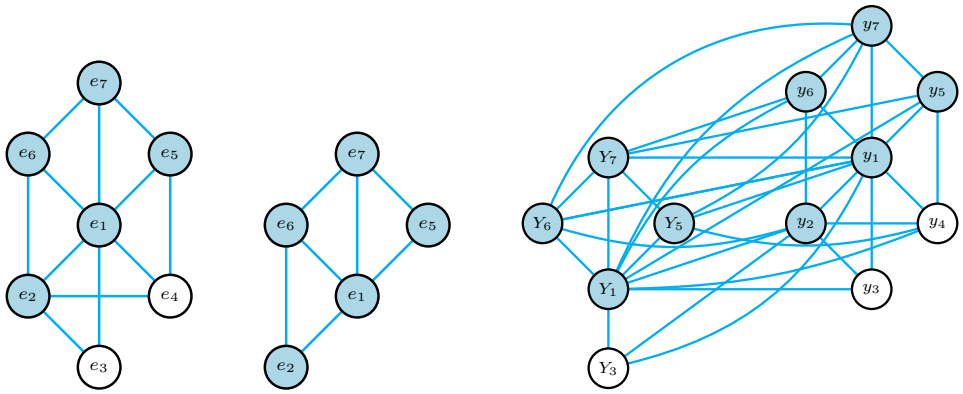

(a) G_c (b) $G_c[E_P]$ (c) G_c^{UT}

Figure 1: Conflict Graphs for Example 5.1
(a) Edge Conflict Graph for U-DT and U-ST; (b) Edge Conflict Graph for LBBD; (c) Variable Conflict Graph for U-DT and U-ST

5.2.1 Edge Conflict Graphs and Clique Inequalities

Edge Conflict Graph G_c and Clique Inequalities for U-DT and U-ST Based on Definition 3, we construct the conflict graph $G_c = (V_c, E_c)$ associated with edges in conflict. Recall in Section 5.1.1 that edges inaccessible for the first traversal E^1 have been eliminated, leaving only edges in the complementary set $E \setminus E^1$. Then, the vertex set V_c consists of one vertex for each edge $e \in E \setminus E^1$. The edge set E_c contains an edge for every pair of distinct vertices $e, e' \in V_c$ such that edges e and e' are in conflict. Formally, the edge conflict graph G_c is defined as:

Definition 4. *The edge conflict graph $G_c = (V_c, E_c)$ is defined by $V_c = \{e \mid e \in E \setminus E^1\}$ and $E_c = \{ee' \mid e, e' \in V_c,\ e \neq e',\ L_{\min}(e, e') > T_{\max}\}$.*

The set of edges in conflict with e will be denoted by N_e, as these edges are neighbors of e in G_c. In Example 5.1, the corresponding edge conflict graph G_c is depicted in Figure 1a. As illustrated, the sets $\{e_1, e_2, e_3\}$, $\{e_1, e_2, e_4\}$, $\{e_1, e_4, e_5\}$, $\{e_1, e_2, e_6\}$, $\{e_1, e_5, e_7\}$, and $\{e_1, e_6, e_7\}$ are maximal cliques in this edge conflict graph.

From G_c, we can derive the following node packing inequalities (see, e.g., Padberg, 1973), which hold trivially and therefore are stated without proof for U-DT:

$$u_e^k + v_{e'}^k \leq 1, \qquad \forall ee' \in E_c,\ k \in K, \tag{12}$$

where u_e^k and $v_{e'}^k$ represent any combination of variables chosen from $\mathbf{s}^k$, $\mathbf{y}^k$, and $\mathbf{Y}^k$ associated with e and e' that are pairwise in conflict. These inequalities ensure that these variables cannot simultaneously take the value one, for any pair of edges in conflict $ee' \in E_c$ and any vehicle $k \in K$. For U-ST, (12) are valid, where u_e^k and $v_{e'}^k$ are chosen from $\mathbf{z}$ (index k omitted), $\mathbf{y}^k$, and $\mathbf{Y}^k$ variables.

The following proposition allows to focus solely on inequalities (12) involving $\mathbf{y}$ variables:

Proposition 5.2. *The node packing inequalities with $\mathbf{y}$ variables*

$$y_e^k + y_{e'}^k \leq 1, \qquad \forall ee' \in E_c,\ k \in K, \tag{13}$$

dominate the other inequalities (12) *for U-DT and U-ST.*

Proof. For U-DT, given inequalities (13), constraints (1g) and (1f) can be used to derive the other node packing inequalities (12) by replacing the $\mathbf{y}$ variables with $\mathbf{s}$ or $\mathbf{Y}$ variables. Similarly, for U-ST, the result follows from inequalities (2b) and (1f). □ □

Thus, the remainder of this section focuses solely on inequalities (13) for U-DT and U-ST.

To strengthen inequalities (13), consider a collection of cliques $\mathcal{U}$ in G_c, where:

- Each clique $U \in \mathcal{U}$ is maximal.
- Every edge in the edge conflict graph $e_c \in E_c$ is contained in at least one clique $U \in \mathcal{U}$.

Such a collection $\mathcal{U}$ is called a *Maximal Clique Cover* (MCC) of G_c. The following result holds:

Proposition 5.3. *(Padberg, 1973) Given an MCC $\mathcal{U}$ of G_c, the following clique inequalities are valid for U-DT and U-ST:*

$$y^k(U) \leq 1, \qquad \forall U \in \mathcal{U},\, k \in K, \tag{14}$$

which are facet-defining for the convex hull of integer solutions of (13) *and can replace* (13)*.*

Consider an MCC $\mathcal{U} = \{\{e_1, e_2, e_3\}, \{e_1, e_2, e_4\}, \{e_1, e_4, e_5\}, \{e_1, e_2, e_6\}, \{e_1, e_5, e_7\}, \{e_1, e_6, e_7\}\}$ for Example 5.1. The associated clique inequalities are $y_1^k + y_2^k + y_3^k \leq 1$, $y_1^k + y_2^k + y_4^k \leq 1$, $y_1^k + y_4^k + y_5^k \leq 1$, $y_1^k + y_2^k + y_6^k \leq 1$, $y_1^k + y_5^k + y_7^k \leq 1$, and $y_1^k + y_6^k + y_7^k \leq 1$, for each $k \in K$.

We now show that inequalities (14) dominate the other clique inequalities with Y or s (z) variables.

Proposition 5.4. *Given an MCC $\mathcal{U}$ of G_c, for each clique $U \in \mathcal{U}$, consider a partition $U = (U_1, U_2, U_3)$ such that $U_1 \subseteq E_P \cap U$, the cliques inequalities for U-DT*

$$s^k(U_1) + y^k(U_2) + Y^k(U_3) \leq 1, \qquad \forall U = (U_1, U_2, U_3) \in \mathcal{U},\, k \in K, \tag{15}$$

are implied by inequalities (14) *and* (1f) *and* (1g)*, for all $k \in K$.*
Similarly, the clique inequalities for U-ST:

$$z(U_1) + y^k(U_2) + Y^k(U_3) \leq 1, \qquad \forall U = (U_1, U_2, U_3) \in \mathcal{U},\, k \in K, \tag{16}$$

are implied by inequalities (14) *and* (1f) *and* (2b)*, for all $k \in K$.*

Proof. For U-DT, given an inequality (15), it can be obtained by summing up inequalities (1g) for all $e \in U_1$, inequalities (1f) for all $e \in U_3$, and the inequality (14) for U. Similarly, for U-ST, given an inequality (16), it can be derived by summing up inequalities (2b) for all $e \in U_1$, inequalities (1f) for all $e \in U_3$, and the inequality (14) for U. □ □

For Example 5.1, this proposition implies that inequalities $s_1^k + y_2^k + Y_3^k \leq 1$ and $z_1 + y_2^k + Y_3^k \leq 1$ are dominated by $y_1^k + y_2^k + y_3^k \leq 1$, for each $k \in K$, and so on.

Note that there is an alternative to constraints (13), given as follows:

Proposition 5.5. *(Della Croce and Tadei, 1994) For an edge in the edge conflict graph $e \in V_c$, the following inequalities are valid for U-DT and U-ST:*

$$|N_e| y_e^k + y^k(N_e) \leq |N_e|, \qquad \forall e \in V_c,\, k \in K. \tag{17}$$

These inequalities are linear combinations of (13), and thus replacing constraints (13) with (17) does not result in a tighter LP relaxation. However, their main advantage is that they reduce the number of constraints from $|K||V_c|^2$ in (13) to $|K||V_c|$ in (17), which can potentially improve computational efficiency.

Edge Conflict Graph $G_c[E_P]$ and Clique Inequalities for LBBD Since LBBD involves only service variables $\mathbf{s}$, we will focus on a subgraph of G_c induced by the vertices that represent profitable edges E_P, denoted by $G_c[E_P] = (V_c[E_P], E_c[E_P])$, where $V_c[E_P]$ represents the set of vertices for profitable edges E_P, and $E_c[E_P]$ contains edges connecting profitable edges E_P in conflict. For Example 5.1, this conflict graph contains only profitable edges e_1, e_2, e_5, e_6, and e_7 as shown in Figure 1b.

The node packing inequalities for LBBD, defined only for the service variables $\mathbf{s}$, are as follows:

$$s_e^k + s_{e'}^k \leq 1, \qquad \forall ee' \in E_c[E_P], k \in K. \tag{18}$$

As in the case of U-DT and U-ST, these inequalities can be replaced by the clique inequalities derived from an MCC of $G_c[E_P]$:

Proposition 5.6. *(Padberg, 1973) Given an MCC $\mathcal{U}$ of $G_c[E_P]$, the following clique inequalities are valid for LBBD:*

$$s^k(U) \leq 1, \qquad \forall U \in \mathcal{U},\, k \in K, \tag{19}$$

which are facet-defining for the convex hull of integer solutions of (18) *and can replace* (18)*.*

For Example 5.1, consider an MCC $\mathcal{U} = \{\{e_1, e_2, e_6\}, \{e_1, e_5, e_7\}, \{e_1, e_6, e_7\}\}$ in $G_c[E_P]$ (Figure 1b). The corresponding clique inequalities (19) are $s_1^k + s_2^k + s_6^k \leq 1$, $s_1^k + s_5^k + s_7^k \leq 1$, and $s_1^k + s_6^k + s_7^k \leq 1$, for $k \in K$.

5.2.2 Variable Conflict Graphs and IS Inequalities

Since the number of maximal cliques in a conflict graph can be exponential (Moon and Moser, 1965), the number of clique inequalities can also be exponential. Considering this, when clique inequalities are not imposed for *all cliques* $U \in \mathcal{U}$ in a given edge conflict graph, one can strengthen the node packing inequalities (13) and (18) by introducing IS inequalities, defined for profitable edges E_P in the variable conflict graph.

Variable Conflict Graph and IS Inequalities for U-ST and U-DT The variable conflict graph is constructed to capture the relationships among decision variables for U-DT and U-ST formulations. The vertices of this graph are associated with the decision variables. Note that service variables $\mathbf{s}$ and $\mathbf{z}$ are excluded since, due to the linking constraints (1g) and (2b), they are *implied* by $\mathbf{y}$ variables. In other words, given a profitable edge $e \in E_P$ and $k \in K$, if y_e^k is in conflict with another variable, the corresponding service variables s_e^k and z_e are also in conflict with the same variable. Therefore, the vertex set V_c^{UT} is associated with $\mathbf{y}$ and $\mathbf{Y}$ variables. Since the vehicles are homogeneous and have the same travel time limit $T_{\max}$, this graph is the same for every vehicle so we drop the vehicle index $k \in K$. Since all our variables are binary, we say that two distinct variables are in conflict if at most one of them can take value one. For each pair of distinct variables in the set V_c^{UT}, if they are in conflict, there is an edge in the graph forming the edge set E_c^{UT}. The formal definition is:

Definition 5. *A variable conflict graph $G_c^{UT} = (V_c^{UT}, E_c^{UT})$ for U-DT and U-ST is defined by $V_c^{UT} = \{y_e \mid e \in E \setminus E^1\} \cup \{Y_e \mid e \in E \setminus (E^1 \cup E^2)\}$ and $E_c^{UT} = \{y_e y_{e'} \mid y_e, y_{e'} \in V_c^{UT},\, e \neq e',\, L_{\min}(e, e') > T_{\max}\} \cup \{Y_e Y_{e'} \mid Y_e, Y_{e'} \in V_c^{UT},\, e \neq e',\, L_{\min}(e, e') > T_{\max}\} \cup \{y_e Y_{e'} \mid y_e, Y_{e'} \in V_c^{UT},\, e \neq e',\, L_{\min}(e, e') > T_{\max}\}$.*

Figure 1c shows the variable conflict graph G_c^{UT} for Example 5.1, with vertex set $\{y_1, ..., y_7, Y_1, Y_3, Y_5, Y_6, Y_7\}$. Vertices associated with profitable edges are shown in blue, while those corresponding to non-profitable edges are depicted in white. Vertices associated with Y_2 and Y_4 have been removed because they cannot be traversed for the second time (i.e., we assumed $E^2 = \{e_2, e_4\}$). The edges in the conflict graph G_c^{UT} connect variables that are in conflict.

We now introduce the IS inequalities in G_c^{UT}, as a generalization and strengthening of inequalities (17) derived from the edge conflict graph G_c (see Proposition 5.5). In this non-trivial and tighter variant of inequalities (17) we are replacing $|N_e|$ with the size of the maximum independent set in the subgraph of G_c^{UT} induced by y_e and its neighbors. We will refer to such obtained cuts as *IS inequalities* (El-Hajj et al., 2016).

Proposition 5.7. *For each $y_e \in V_c^{UT}$ where $e \in E_P$, let α_e^V be the size of the maximum independent set in the subgraph of G_c^{UT} induced by y_e and its neighbors. Recall that N_e is the set of edges in conflict with e. Then, the following IS inequalities are valid for U-DT and U-ST:*

$$\alpha_e^V y_e^k + y^k(N_e) + Y^k(N_e \setminus E^2) \leq \alpha_e^V, \qquad \forall y_e^k \in V_c^{UT},\, e \in E_P,\, k \in K. \tag{20}$$

Proof. To verify the inequalities are valid, it suffices to show that the set $\{y_{e'} \mid e' \in N_e\} \cup \{Y_{e'} \mid e' \in N_e \setminus E^2\}$ represents the neighbors of y_e in G_c^{UT}. This follows directly from the definition of N_e as the set of edges in conflict with e. □ □

Consider Example 5.1. For y_1, the set of edges in conflict with e_1 is $N_{e_1} = \{e_2, \ldots, e_7\}$ and $N_{e_1} \setminus E^2 = \{e_3, e_5, e_6, e_7\}$. Thus, the set of neighbors of y_1 in G_c^{UT} is $\{y_2, ..., y_7, Y_3, Y_5, Y_6, Y_7\}$ and the corresponding size of maximum independent set is $\alpha_{e_1}^V = 6$. Then the IS inequalities (20) for y_1 are $6y_1^k + y_2^k + y_3^k + y_4^k + y_5^k + y_6^k + y_7^k + Y_3^k + Y_5^k + Y_6^k + Y_7^k \leq 6$, for all $k \in K$. These inequalities (one per each vehicle) ensure that if variable y_1^k is set to one, all the neighboring variables of y_1 in G_c^{UT} must be set to zero. Otherwise, at most six among these neighbors can be set to one.

Variable Conflict Graph and IS Inequalities for LBBD The variable conflict graph for LBBD with service variables $\mathbf{s}$, coincides with the edge conflict graph $G_c[E_P]$, where the vertices representing profitable edges E_P are replaced by the service variables $\mathbf{s}^k$ for each vehicle $k \in K$.

The IS inequalities for LBBD, derived from the edge conflict graph $G_c[E_P]$ are as follows:

Proposition 5.8. *For a profitable edge in the edge conflict graph $e \in V_c[E_P]$, let α_e^E be the size of the maximum independent set in the subgraph of $G_c[E_P]$ induced by e and $N_e \cap E_P$. Then, the following IS inequalities are valid for LBBD:*

$$\alpha_e^E s_e^k + s^k(N_e \cap E_P) \leq \alpha_e^E, \qquad \forall e \in V_c[E_P],\, k \in K. \tag{21}$$

For the edge e_1 in Example 5.1, the set of edges in conflict $N_{e_1} \cap E_P$ is $\{e_2, e_5, e_6, e_7\}$ and the size of maximum independent set in the subgraph of $G_c[E_P]$ induced by e_1 and its neighbors is $\alpha_{e_1}^E = 2$. Thus, the IS inequalities (21) for e_1 are $2s_1^k + s_2^k + s_5^k + s_6^k + s_7^k \leq 2$, for all $k \in K$.

5.2.3 Remarks

Comparison of Clique and IS Inequalities from Edge and Variable Conflict Graphs For the UTOARP, although clique and IS inequalities can be derived from both *edge* and *variable* conflict graphs, we focus on clique inequalities derived from edge conflict graphs and IS inequalities derived from variable conflict graphs. Since, in UTOARP formulations, each edge corresponds to multiple decision variables (service variables $\mathbf{s}$ and $\mathbf{z}$, traversal variables $\mathbf{y}$ and $\mathbf{Y}$), variable conflict graphs are inherently more complex than edge conflict graphs. For clique inequalities, cliques in edge conflict graphs are easier to identify and analyze compared to those in variable conflict graphs. More importantly, for the proposed formulations U-DT and U-ST, as shown in Proposition 5.9 below, the clique inequalities derived from edge conflict graphs (and using only $\mathbf{y}$ variables) dominate those from variable conflict graphs. Moreover, for LBBD, the clique inequalities from edge and variable conflict graphs are identical. Conversely, for IS inequalities, working on variable conflict graphs is more efficient since these graphs explicitly represent all related decision variables and their neighborhood structures. To mitigate the analytical and computational challenges of variable conflict graphs, in our implementation, IS inequalities are derived only for profitable edges.

The following proposition establishes that the clique inequalities from G_c^{UT} are dominated by those derived from G_c.

Proposition 5.9. *Given a clique $U^{UT} = (U_y^{UT}, U_Y^{UT})$ in the variable conflict graph, where U_y^{UT} and U_Y^{UT} represent the set of $\mathbf{y}$ and $\mathbf{Y}$ variables in this clique, there exists a corresponding clique U in the edge conflict graph G_c such that the clique inequalities for U^{UT}:*

$$\sum_{y \in U_y^{UT}} y^k + \sum_{Y \in U_Y^{UT}} Y^k \leq 1, \qquad \forall k \in K, \tag{22}$$

are implied by the clique inequalities for U: $y^k(U) \leq 1$, $\forall k \in K$.

Proof. By the definition of the variable conflict graph G_c^{UT}, for any edge $e \in E$, the associated variables y_e^k and Y_e^k cannot both exist in U^{UT}. This implies that the edges associated with the variables in U^{UT} are distinct and in conflict with each other. Consequently, these edges form a clique U in the edge conflict graph G_c. From Proposition 5.4, it follows that inequalities (22) are implied by the clique inequalities for U with $\mathbf{y}$ variables. □ □

Construction of Variable Conflict Graphs In this section, we have presented one way to construct the variable conflict graph and derive valid clique and IS inequalities for formulations U-DT/U-ST, based on our knowledge and understanding of this problem. There may exist alternative ways to define the variable conflict graph. For example, one could build a conflict graph that includes all decision variables, in which case potentially different inequalities could be derived.

5.3 Symmetry Breaking Constraints

To eliminate symmetric solutions, we use the following three symmetry breaking rules. Specifically, the first two are adapted from Archetti et al. (2014) for the directed TOARP. We derive the third one from a property of the undirected graph G. These properties need not be satisfied by all feasible solutions, but there is at least one optimal solution that satisfies them. Below we assume that profitable edges have been sorted according to some order, so e_t denotes the t-th profitable edge.

(SB1) No profitable edge e_t is served by a vehicle with an index larger than its own index.

(SB2) If a profitable edge e_t is served by the vehicle k, then there exists at least one profitable edge with a smaller index served by vehicle $k-1$.

(SB3) If a profitable edge e is traversed by several vehicles, then it is served by the vehicle with the smallest index.

The rules SB1-SB3 do not conflict with each other so they can be applied simultaneously.

The application of these rules varies across different formulations: For U-DT, SB1-SB3 can be represented as follows:

$$\text{(SB1)} \qquad s^k_{e_t} = 0, \qquad \forall e_t \in E_P,\ t \in \{1,...,|K|-1\},\ k \in \{t+1,...,|K|\}, \tag{23a}$$

$$\text{(SB2)} \qquad s^k_{e_t} \leq \sum_{q=k-1}^{t-1} s^{k-1}_{e_q}, \qquad \forall k \in \{2,...,|K|\},\ t \in \{k,...,|E_P|\}, \tag{23b}$$

$$\text{(SB3)} \qquad y^k_e \leq \sum_{k'=1}^{k} s^{k'}_e, \qquad \forall e \in E_P,\ k \in K. \tag{23c}$$

Note that with (23a), the summation of $s^k_{e_q}$ on the right-hand-side of (23b) can start from $q = k-1$ instead of $q = 1$ since $t \geq k$. For U-ST, we cannot represent rules SB1-SB3 using the aggregated service variables z. Instead, we present the alternative rules applicable to U-ST in Appendix A.2. For LBBD, we can only use (23a)-(23b) since it contains service variables $\mathbf{s}$ only.

5.4 Strengthened Logic-Based Benders Cuts

The SLBBCs (7b) can serve as Benders feasibility cuts to discard IPSs in the LBBD, but they can also be used as valid inequalities for U-DT and U-ST. By the definition of IPS, the edges in H cannot be traversed, hence we can use first-traversal variables $\mathbf{y}$ in the SLBBCs:

$$\sum_{e \in H} y^k_e \leq |H| - 1, \qquad \forall k \in K,\ H \subseteq E_P \text{ irreducible IPS}. \tag{24}$$

6 Heuristics and Separation Procedures

In this section, we describe methods for separating and generating valid inequalities, along with the heuristics used to enhance the performance of the exact algorithms. We begin with the detailed procedure for solving the URPP in Section 6.1, as it forms the foundation for the subsequent separation methods and heuristics. In Section 6.2, we discuss procedures for separating the SLBBCs, connectivity constraints, and co-circuit inequalities. We also explain how we generate clique and IS inequalities. In Section 6.3, we present a MIP start heuristic for identifying initial feasible solutions.

6.1 Solving the URPP

The starting point of our heuristics and the SLBBC separation procedure is a subset of profitable edges associated with every vehicle $k \in K$, such that no two vehicles serve the same profitable edge. That is, we are given a set of binary vectors $\bar{\mathbf{s}}^k$, one associated with each vehicle $k \in K$, such that the subsets $P(\bar{\mathbf{s}}^k)$ are pairwise disjoint and $\cup_{k \in K} P(\bar{\mathbf{s}}^k) \subseteq E_P$. In order to check feasibility, we need to determine whether for

a given set of binary vectors $\bar{\mathbf{s}}^k$, $k \in K$, each vehicle can complete a tour within $T_{\max}$. In order to do so, we need to solve an instance of the URPP, one for each $k \in K$, with the set $P(\bar{\mathbf{s}}^k)$ representing the set of required edges.

Numerous formulations and algorithms exist for solving the URPP (see, Ghiani and Laporte, 2015). However, most of them require graph transformations and preprocessing procedures. Applying these approaches can be computationally inefficient when solving the URPP repeatedly, each time with a modified set of required edges, as it is the case in our Branch-and-Benders-cut implementation. This is why we opt for solving an ILP model (based on a B&C procedure) as a "black-box" solution procedure for the URPP. Our ILP formulation utilizes binary variables for the first and second deadheads, and avoids graph transformation. The formulation is provided in Appendix B.1.

To speed up the solution procedure of the URPP, we feed a feasible solution to the ILP model as an initial starting point. The specifics of how this initial solution is generated will be outlined in each of the heuristics discussed in this section. Additionally, since the LBBD subproblem is a feasibility problem, we immediately stop the solution procedure if the lower bound of the URPP obtained by the ILP formulation exceeds the travel time limit $T_{\max}$ or the upper bound is smaller than or equal to $T_{\max}$. Since the number of required edges assigned to each vehicle is much smaller than in typical benchmark URPP instances, we observed that the separation of SLBBCs using the proposed ILP model and a nested B&C procedure did not impose a significant computational burden.

6.2 Separation and Cut Generation Procedures

6.2.1 Separation of Strengthened Logic-Based Benders Cuts

In order to guarantee validity of our LBBD, it is necessary to have a procedure that separates LBBCs *exactly*. A rudimentary separation of the LBBCs would be to directly solve a URPP for each vehicle $k \in K$ with the set of required edges given by $\bar{\mathbf{s}}^k$. We use a B&C procedure to solve the URPP exactly (see Appendix B.1 for further details). This procedure can be interrupted whenever (1) a feasible solution is found whose tour length does not exceed $T_{\max}$ (indicating that $\bar{\mathbf{s}}^k$ is a feasible assignment), or (2) a global lower bound of the given URPP instance exceeds $T_{\max}$, indicating that $\bar{\mathbf{s}}^k$ induces an IPS.

To improve the efficiency, we apply several algorithmic enhancements, and resort to this rudimentary approach only if necessary. First of all, we are interested in deriving stronger Benders cuts, preferably irreducible ones. Since this is a difficult task, we apply a (lifting) heuristic that finds RIPS and down-lifts coefficients of the violated Benders feasibility cut. Moreover, while searching for possible violated Benders cuts, as a byproduct, we also generate a feasible UTOARP solution. The pseudocode of this procedure is given in Algorithm 1. The feasible solution ψ returned by the algorithm is represented as a union of edges (H^k, L^k) over all $k \in K$, i.e., $\psi = \cup_{k \in K} \psi^k = \cup_{k \in K} (H^k, L^k)$, where $H^k \subseteq E_P$ represents the edges served by vehicle k, and $L^k \subseteq E$ stands for the edges deadheaded by vehicle k. The auxiliary set $\mathcal{H}$ contains all edges that will be served by the feasible solution. We provide a brief overview of Algorithm 1 below, with detailed explanations available in Appendix B.2.

In a nutshell, given the set of required edges defined by $\bar{\mathbf{s}}^k$, namely $H^k = \{e \in E_P \mid \bar{s}_e^k = 1,\ e \in E_P\}$:

1. We first apply a simple path-insertion heuristic (see lines 3-8 of Algorithm 1) that finds a tour containing all the edges from H^k. If the length of this tour does not exceed $T_{\max}$, no Benders cut is needed and the tour (H^k, L^k) is stored to create a feasible solution (see lines 9-11 of Algorithm 1).

2. Otherwise, for the set of edges from H^k, we call the B&C procedure to solve the corresponding URPP instance exactly. If the length of the resulting URPP tour does not exceed $T_{\max}$, no Benders cut is needed and the resulting URPP tour (H^k, L^k) is stored to create a feasible solution (see lines 12-14 of Algorithm 1).

3. Otherwise, the set H^k corresponds to an IPS, and we iteratively remove edges from H^k until a feasible tour is found – this tour is stored to create a feasible solution (see line 16 of Algorithm 1). The last removed edge is then reinserted, to generate a RIPS for which a violated Benders cut is generated (see line 17 of Algorithm 1).

4. In order to solve the URPP more efficiently, we initialize the B&C URPP procedure with a tour found using the path-insertion heuristic (see line 12 of Algorithm 1).

We notice that feasible tours are found independently for each $k \in K$. They are then merged into a feasible solution to which a local improvement heuristic is applied (see lines 19-21 of Algorithm 1). Algorithm 1 is called at every node of the branching tree, each time a binary solution $\bar{\mathbf{s}}$ is found. Overall, the algorithm guarantees the exact separation of Benders cuts while enhancing both the efficiency and effectiveness of the decomposition approach.

Algorithm 1: Separation of Strengthened Logic-based Benders Cuts

Input: the time limit $T_{\max}$, an integer solution $\bar{\mathbf{s}}$ of the current RMP
Output: Benders cuts to be inserted into the RMP, and a feasible solution to the UTOARP ψ

1 $\mathcal{H} \leftarrow \emptyset$, $\psi \leftarrow \emptyset$;
2 **for** $k \in K$ **do**
3 $\quad H^k \leftarrow \{e \in E_P \mid \bar{s}_e^k = 1,\ e \in E_P\}$, $\bar{H}^k = \emptyset$, $\bar{\psi}^k \leftarrow \emptyset$, $\bar{\tau}^k \leftarrow 0$, $\mathcal{V}_{\bar{H}^k} \leftarrow \{0\}$;
4 $\quad$ **repeat** `// Path-insertion Heuristic to construct a solution to the URPP`
5 $\quad\quad$ **for** $e \in H^k$ **do**
6 $\quad\quad\quad$ **if** $e \notin \bar{H}^k$ **then** $l_e = \min_{i \in \mathcal{V}_{\bar{H}^k}} l_{ie}^1$, $i_e \in \arg\min_{i \in \mathcal{V}_{\bar{H}^k}} l_{ie}^1$;
7 $\quad\quad$ Choose the edge $e' = i'j' \in \arg\min_{e \in H^k \setminus \bar{H}^k} l_e$, and let $\bar{H}^k \leftarrow \bar{H}^k \cup \{e'\}$, $\bar{\psi}^k \leftarrow \bar{\psi}^k \cup (e', L_{i_{e'}e'})$, $\bar{\tau}^k \leftarrow \bar{\tau}^k + l_{e'}$, $\mathcal{V}_{\bar{H}^k} \leftarrow \mathcal{V}_{\bar{H}^k} \cup \{i'\} \cup \{j'\}$;
8 $\quad$ **until** $\bar{H}^k = H^k$;
9 $\quad$ **if** $\bar{\tau}^k \le T_{\max}$ **then** `// ` H^k `is an FPS by the constructed solution`
10 $\quad\quad$ Update $\mathcal{H} \leftarrow \mathcal{H} \cup H^k$, $\psi^k \leftarrow \bar{\psi}^k$;
11 $\quad$ **else** `// Evaluate the feasibility of` H^k `by solving the URPP`
12 $\quad\quad$ Solve an instance of the URPP of H^k with $\bar{\psi}^k$ as an initial feasible solution, and let $T^*(H^k)$ be the returned objective value;
13 $\quad\quad$ **if** $T^*(H^k) \le T_{\max}$ **then** `//` H^k `is an FPS`
14 $\quad\quad\quad$ Record the feasible solution $\psi^k = (H^k, L^k)$ from the URPP ;
15 $\quad\quad$ **else** `//` H^k `is an IPS`
16 $\quad\quad\quad$ Call `Find_a_RIPS`$(H^k, \bar{\psi}^k, T_{\max})$. Let $\hat{H}^k$ be the obtained RIPS, and let $\psi^k = (H^k, L^k)$ be the returned feasible solution to the tour k (See Algorithm 2);
17 $\quad\quad\quad$ Store the cuts (7b) or (24) for $\hat{H}^k$;
18 $\quad\quad$ Update $\mathcal{H} \leftarrow \mathcal{H} \cup H^k$;
19 **for** $k \in K$ **do** `// Improvement Heuristic`
20 $\quad$ **for** $e \in E_P \setminus \mathcal{H}$ **do**
21 $\quad\quad$ **if** $e \in L^k$ **then** $H^k \leftarrow H^k \cup \{e\}$, $L^k \leftarrow L^k \setminus \{e\}$, $\psi^k \leftarrow (H^k, L^k)$, $\mathcal{H} \leftarrow \mathcal{H} \cup \{e\}$;
22 Return the Benders cuts (7b) or (24) for $\hat{H}^k$ for each $k \in K$, and a feasible UTOARP solution $\psi = \bigcup_{k \in K} \psi^k$.

6.2.2 Separation of Connectivity Constraints

Connectivity constraints (1e) are commonly used in the ARPs literature and they can be separated in polynomial time. At integer points, the separation procedure reduces to finding the connected components of the support graph whose edges are determined by the current solution. At fractional points, one builds an auxiliary graph and sets the capacity of each edge in this graph equal to the value of the left-hand-side in the constraints (i.e., $y_e + Y_e$). Then one needs to find the max-flow/min-cut between the depot and each vertex. For details, we refer to the Section 7.4 of Dror (2000).

6.2.3 Separation of Co-circuit Constraints

To separate co-circuit constraints (1d), one rewrites them so that all variables appear in the left-hand-side and the right-hand-side only contains the constant term 1. For integer points, it is enough to check the violation for singletons. For fractional points, one needs to construct an auxiliary graph where edge capacities are

based on the value of the left-hand-side in the constraints for the solution. The tree of min-cuts between pairs of vertices in the auxiliary graph (Gusfield, 1990) allows to detect whether there exists a vertex set S that violates these constraints. Details of the implementation procedure can be found in Aráoz et al. (2009).

6.2.4 Generation of Clique Inequalities

We generate clique inequalities ((14) for U-DT and U-ST, and (19) for LBBD), to initialize the formulations before starting the branching procedure. Specifically, we identify two MCCs, namely the maximum *cardinality* MCC where each clique is obtained by solving a *Maximum Clique Problem* (MCP), and the maximum *weight* MCC where each clique is identified by solving a *Maximum Weight Clique Problem* (MWCP, see, e.g., Bomze et al., 1999), where the weight is $r_e + 1$ for profitable edges $e \in E_P$ and 1 for non-profitable edges $e \in E_{NP}$. All cliques are generated on the edge conflict graph G_c for U-DT and U-ST and on the edge conflict graph $G_c[E_P]$ for LBBD.

To efficiently find an MCC of a given edge conflict graph, we propose the following heuristic: we rank the edges ($e_c = ee' \in E_c$ or $E_c[E_P]$) in the edge conflict graph based on the total profits associated with their end-vertices (i.e., $r_e + r_{e'}$). Starting with the most profitable edge e'_c, we solve an MCP or MWCP with the constraint that this edge e'_c must be included in the clique. Once a clique is identified, the next most profitable edge not yet included in any clique is selected, and another MCP or MWCP is solved under the same inclusion constraint. This process continues until every edge in the edge conflict graph is included in at least one clique. The formulations for the MCP and the MWCP used in each iteration are provided in Appendix B.3.

6.2.5 Generation of Independent Set Inequalities

The IS inequalities are also used to initialize the proposed formulations. Specifically, for U-DT and U-ST, inequalities (20) are generated for each first-traversal variable y_e^k for each profitable edge $e \in E_P$ and each vehicle $k \in K$. For LBBD, inequalities (21) are added for each service variable s_e^k corresponding to each profitable edge $e \in E_P$ and each vehicle $k \in K$. To obtain these inequalities, we need to determine the size of the maximum independent set α: 1) for the given decision variable $y_e \in V_c^{UT}$ in the variable conflict graph G_c^{UT} for U-DT and U-ST; 2) for the given profitable edge $e \in E_P$ in the edge conflict subgraph $G_c[E_P]$. This requires solving a Maximum Independent Set Problem (MISP), for which we use the edge formulation for the MCP (see, e.g., Bomze et al., 1999).

6.3 MIP Start Heuristic

To generate initial feasible solutions for the problem, we develop a greedy randomized heuristic. This heuristic is inspired by the greedy randomized adaptive search procedure (GRASP, Feo and Resende, 1995) and the classic greedy heuristic for the knapsack problem (Dantzig, 1957). The idea is to construct a feasible tour for each vehicle by sequentially selecting a profitable edge from a set of good candidates, determined in a greedy and randomized manner. After constructing the tour, in order to select more profitable edges, an instance of the URPP is solved using the selected candidates as required edges. Finally, a local improvement is applied to serve additional edges traversed by a tour, but not served so far. The pseudocode and explanations are provided in Appendix B.4.

7 Computational results

We implemented B&C approaches for the three proposed formulations, and in this section we empirically compare them. We also investigate how the proposed heuristics and valid inequalities affect their computational performance. As a benchmark, we have also implemented a compact, load-based formulation (referred to as D-DL) presented in Appendix C. We first introduce the dataset and test settings in Section 7.1. Then, we compare the performance of the basic formulations in Section 7.2. Following this, we apply the MIP start heuristic (see Section 6.3) and proposed valid inequalities (see Section 5), and evaluate their impact on the formulations' performance in Sections 7.3 and 7.4, respectively. In Appendix D.3, we examine the performance of the formulations under varying travel time limits and number of vehicles to assess scalability.

Formulation	Variables	Constraints	Size	Method
U-DT	s, y, Y	(1)	exponential	B&C
U-ST	z, y, Y	(2)	exponential	B&C
LBBD	s	(7a), (7c), (5)	exponential	B&C
D-DL	s, x, f	(30)	compact	B&B

Table 2: Setting of Basic Formulations

7.1 Dataset and Test Setting

The benchmark instances used in the computational tests are adapted from the 118 instances for the Prize-Collecting Rural Postman Problem in Aráoz et al. (2009). The profits for the profitable edges have been obtained as indicated in the original paper. In each instance, the original *required* edges are considered *profitable* edges in our case, thus retaining their associated profits. Conversely, profits for the *non-required* edges are discarded. We further divide the instances into two groups based on the number of vertices. Instances with fewer than 90 vertices (11 sets, 98 instances) are classified as *small* instances, while the remaining instances (4 sets, 20 instances) are *large* instances. Detailed information about these instances is provided in Appendix D.1.

Two critical parameters that influence the difficulty of the instances are the number of vehicles $|K|$ and the travel time limit $T_{\max}$. For the number of vehicles, we consider $|K| = \{3, 4, 5\}$. Setting the travel time limit $T_{\max}$ is more complex (see Archetti et al., 2014). We define it as $T_{\max} = \beta T_{base}$, where $T_{base} = \frac{|E_{NP}|}{|E_P||K|} \sum_{e \in E_P} t_e$ serves as a base value, influenced by the ratio of non-profitable edges to total edges and the number of vehicles. We test the formulations' performance with $\beta \in \{0.6, 0.8, 1.0\}$.

All algorithms are coded in C++ with Visual Studio 2022, running on a computer with Intel Core i7-12700K (3.6GHz) with 64GB RAM. We use Cplex 22.10 as the solver with concert technology, employing a single thread with default parameters. For the B&C algorithms, we use the lazy constraint callback for separations at integer points, the user cut callback for separations at fractional points (with a cut violation threshold of 0.6), the heuristic callback to return feasible solutions, and the MIPinfo callback to obtain the current dual bounds. The initial feasible solutions are provided using the MIPstart command. The time limits for the tests are 3600 seconds for *small* instances and 7200 seconds for *large* instances. The detailed results are available at `https://github.com/Anonymous`.

7.2 Comparison of Basic Formulations

In this series of tests, we compare the performance of the basic formulations, specifically the original formulations without any heuristics or additional valid inequalities. The detailed settings are presented in Table 2. The original connectivity constraints (1e) and co-circuit constraints (1d) are separated at both integer and fractional points, while the basic logic-based Benders cuts (5) are separated only at integer points. All tests are conducted with $|K| = 4$ and $\beta = 0.8$. To evaluate the performance of these formulations, we compare the number of instances solved to optimality. Additionally, the instances are divided into two sets based on the results: (a) instances that are solved to optimality by all formulations, and (b) instances where at least one formulation does not reach optimality. For set (a), we consider the number of nodes branched at termination and the runtime. For set (b), we report the final gap at termination.

The computational results for small and large instances are summarized in Table 3. For each group (small/large) of instances, the table reports the number of instances solved to optimality within the time limit over the number of all instances (row #Optimal). The instances are then divided into two sets: (a) and (b). The number of instances in each set is indicated in parentheses after the set name. For instances in set (a), the table shows the average runtime in seconds (row Time (s)) and the average number of nodes branched (row #Nodes). For instances in set (b), the table presents the average gap in percentage at the termination (row Gap (%)). The final gap is calculated as the difference between the upper and lower bounds relative to the upper bound (i.e., $Gap = \frac{UB-LB}{UB} \times 100\%$), with a tolerance gap set at 0.01%. If a formulation cannot provide a non-trivial feasible solution (i.e., $LB = 0$), we set the gap to 100%.

For small instances, all formulations solve the majority of instances to optimality within the time limit of 3600s. The LBBD formulation performs the best in terms of the number of instances solved to optimality, the

Group	Metrics		U-DT	U-ST	LBBD	D-DL
Small	Set (a) (66/98)	#Optimal	78/98	76/98	**86/98**	68/98
		Time (s)	35.19	77.45	**27.81**	74.71
		Nodes	8456	8541	**490**	21935
	Set (b) (32/98)	Gap (%)	**17.49%**	26.29%	22.40%	17.87%
Large	Set (b) (20/20)	#Optimal	0/20	0/20	**2/20**	1/20
		Gap (%)	54.85%	64.71%	68.36%	**16.12%**

Table 3: Performance of Basic Formulations

average runtime, and the number of nodes branched for instances in set (a). This efficiency can be attributed to significant fewer binary variables used in LBBD. For the undirected formulations, the disaggregated formulation U-DT shows advantages over the other formulations with respect to the average gap for instances in set (b). The semi-aggregated formulation U-ST, which aggregates service variables, performs slightly worse than U-DT, showing that the aggregation does not yield significant benefits. For the directed formulation D-DL, although it solves the fewest instances to optimality, it maintains a competitive average gap at termination for instances in set (b), just 0.38% worse than U-DT's. This performance can be explained by D-DL being a compact formulation, providing the solver with full information from the start, which allows the solver to use sophisticated bounding and reduction techniques as well as heuristics. In contrast, the other formulations have an exponential number of constraints, which are dynamically generated, hence most of these solver techniques are disabled, and the upper bound is improved throughout the B&C process. However, it should be noted that D-DL produces significantly more branching nodes (over 20,000 on average) compared to the other formulations for instances in set (a), that need fewer than 9,000 nodes on average. This aligns with the fact that directed formulations typically involve more binary variables, resulting in a larger B&B tree.

For large instances, however, all formulations fail to solve the majority of instances to optimality within the 7200s time limit and all the instances are in set (b). LBBD and D-DL perform best, solving two and one instances to optimality, respectively. D-DL maintains a much lower average gap (16.12% versus over 50% for the others), which again can be explained by D-DL's compact structure. The aggregation of service variables in U-ST offers no advantage over the disaggregated U-DT, as U-ST performs much worse in terms of the average gap. None of these two formulations can solve any instance to optimality.

Based on these results, we conclude that all formulations struggle with large instances, with most failing to solve any instances to optimality and producing large average gaps at termination. To improve performance, we explore enhancing the lower bound with initial feasible solutions from a MIP start heuristic and improving the upper bound by incorporating valid inequalities. Given that U-ST is consistently outperformed by U-DT, we exclude U-ST from further tests.

7.3 Effect of MIP Start Heuristic

In this set of tests, we evaluate the effect of the MIP start heuristic, which provides an initial feasible solution (see Section 6.3). The solution is set as a MIPstart for Cplex. The test time consists of two phases: 1) running the MIP start heuristic for 50 times for the *small* instances and 100 times for the *large* instances, where the best solution(s) are retained; and 2) allowing Cplex to run for the remainder of the time to find an optimal solution or reach the time limit. The MIP start heuristic time is consistent across all formulations for the same $|K|$ and $T_{\max}$ values.

Table 4 presents the results of each basic formulation with MIP start heuristic (Formulation+MH), following the same structure as Table 3.

For small instances, the LBBD formulation solved two additional instances to optimality, and the average gap for instances in set (b) decreased by more than 7% after applying the MIP start heuristic. For the other formulations, the impact of the MIP start heuristic is less pronounced. This outcome aligns with theoretical expectations: since LBBD includes only service variables and Benders cuts are separated only at integer solutions, the initial feasible solution has a more substantial impact on LBBD's performance compared to the other formulations.

Group	Metrics		U-DT+MH	LBBD+MH	D-DL+MH
Small	Set (a) (69/98)	#Optimal	77/98	**88/98**	70/98
		Time (s)	53.49	**28.68**	149.26
		Nodes	8035	**839**	39461
	Set (b) (29/98)	Gap (%)	17.90%	**13.99%**	18.71%
Large		#Optimal	0/20	1/20	1/20
	Set (b) (20/20)	Gap (%)	37.36%	46.69%	**18.16%**

Table 4: Performance of Basic Formulations with MIP Start Heuristic

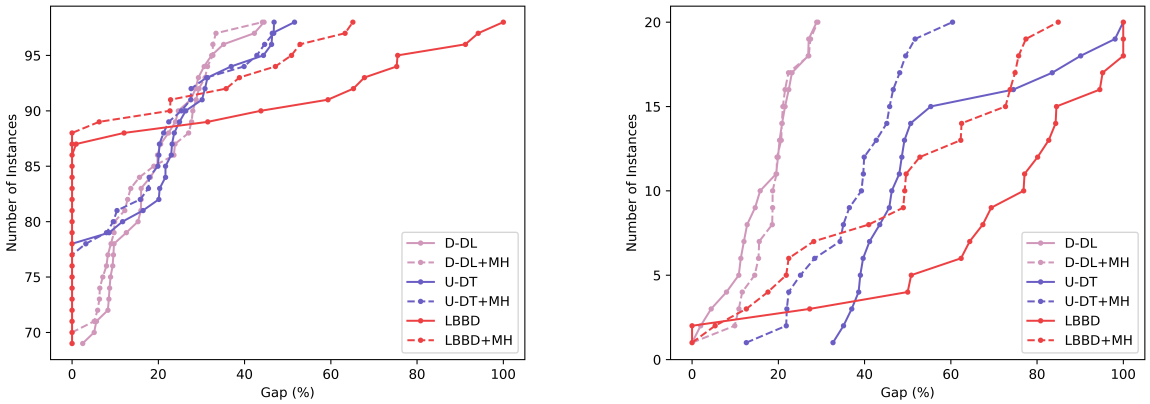

(a) Small Instances

(b) Large Instances

Figure 2: Gap at Termination of Basic Formulations with MIP Start Heuristic

For large instances, although the number of instances solved to optimality remain unchanged, the MIP start heuristic leads to a significant drop in the average gap for instances in set (b) for formulation U-DT and LBBD compared to Table 3. Specifically, the gap reduces by 17.49% for U-DT and 21.67% for LBBD, respectively. In contrast, the MIP start heuristic has minimal effect on the average gap for D-DL. This can be attributed to the compact nature of D-DL, which allows the solver to leverage its internal heuristics more effectively for performance improvement. To further compare performance, Figures 2a and 2b display the empirical cumulative distribution functions (ECDFs) with respect to gap at termination for small and large instances, respectively. These figures illustrate the number of instances (vertical axis) where the gap at termination is less than or equal to the value indicated on the horizontal axis. In these figures, the gaps of basic formulation without MIP start heuristic (label Formulation) are depicted in *solid* lines and the gaps of basic formulation with MIP start heuristic (label Formulation+MH) are in *dashed* lines. For small instances (Figure 2a), the LBBD formulation with the heuristic significantly improves the worst-case gap, reducing it from over 90% to under 70%. For other formulations, the differences are less pronounced. For large instances (Figure 2b), as we observed in Table 4, the MIP start heuristic helps formulations U-DT and LBBD reduce the gap, but has little effect on D-DL.

In conclusion, the MIP start heuristic notably enhances the performance of LBBD for both small and large instances, and the gap for large instances in other formulations without negatively impacting other metrics. Overall, the heuristic proves to be beneficial and is therefore retained in the algorithms.

7.4 Effect of Valid Inequalities

Following the previous results, we now examine the effect of valid inequalities (VI) on the formulations. We refer to the enhanced versions as strengthened formulations. The detailed settings are presented in Table 5.

All the valid inequalities developed in Section 5 can also be adapted to D-DL. Details are provided in

Formulation	Variables	Constraints	Size	Method
U-DT+VI	s, y, Y	(1), (8), (11), (14), (20), (23a)-(23c), (24)	exponential	B&C
LBBD+VI	s	(7), (10), (19), (21), (23a)-(23b)	exponential	B&C
D-DL+VI	s, x, f	(30), (31), (32), (34), (35), (36), (37)	exponential	B&C

Table 5: Setting of Strengthened Formulations

Appendix C.3. In particular, due to the additional constraints (37), the directed formulation D-DL now has an exponential number of constraints and thus has to be solved with a B&C method. The inaccessible traversal inequalities (8), (11), (10), (31), and (32), along with clique inequalities (14), (19), and (34), IS inequalities (20), (21), and (35), and symmetry breaking constraints (23a)-(23c), (23a)-(23b), and (36) are added in the initial formulations before branching, while the SLBBCs (24), (7b), and (37) are separated at the integer points.

As we keep the MIP start heuristic, the algorithms consist of three phases: 1) the MIP start heuristic (Section 7.3); 2) generating the initial clique and IS inequalities (Sections 6.2.4 and 6.2.5); and 3) running Cplex to find an optimal solution or reach the time limit. Note that the generation time for the clique and IS inequalities varies for each formulation, even with the same $|K|$ and $T_{\max}$.

The results of the strengthened formulations with MIP start heuristic (Formulation+VI+MH) for small and large instances are presented in Table 6.

Group	Metrics		U-DT+VI+MH	LBBD+VI+MH	D-DL+VI+MH
Small	Set (a) (87/98)	#Optimal	95/98	**96/98**	87/98
		Time (s)	5.86	**4.18**	15.96
		Nodes	**12**	13	2145
	Set (b) (11/98)	Gap (%)	**2.48%**	3.37%	7.96%
Large	Set (a) (2/20)	#Optimal	8/20	**15/20**	2/20
		Time (s)	11.41	12.33	**11.40**
		Nodes	0	0	0
	Set (b) (18/20)	Gap (%)	10.88%	**5.75%**	10.20%

Table 6: Performance of Strengthened Formulations with MIP Start Heuristic

For small instances, there is a clear improvement compared to Table 4. The number of instances solved to optimality increases significantly, with U-DT, LBBD, and D-DL solving 18, 8, and 17 more instances, respectively. This improvement brings U-DT to a competitive level with LBBD, while D-DL, though improved, still lags behind the other two. The number of branching nodes for instances in set (a) decreases notably for all formulations: U-DT (-8,023), LBBD (-826), and D-DL (-37,316). However, D-DL continues to branch far more nodes due to its higher binary variable count. In terms of average runtime for instances in set (a), LBBD shows a slight advantage (4.18 seconds), followed by U-DT (5.86 seconds), with D-DL remaining the slowest (15.96 seconds). The average gap for instances in set (b) falls below 10% for all formulations, with U-DT achieving the smallest gap (2.48%), followed by LBBD (3.37%) and D-DL (7.96%).

For large instances, there is a similar improvement compared to Table 4. LBBD continues to lead in the number of instances solved to optimality, increasing by 14 (15/20), while U-DT solves 8 more instances, narrowing the gap with LBBD. D-DL sees modest improvement, solving 1 more instance. The average runtime and the number of nodes branched are comparable across all three formulations, indicating similar computational effort in solving the instances in set (a). Average gap for instances in set (b) improves significantly, with LBBD showing the lowest (5.75%), closely followed by D-DL (10.20%) and U-DT (10.88%).

In the following, we present the ECDFs with respect to the gap at termination in Figure 3. The strengthened formulations with MIP start heuristic (Formulation+VI+MH) are represented by *solid* lines with *triangle* markers, while the basic formulations with MIP start heuristic (Formulation+MH) are depicted by *dashed* lines with *dot* markers. In Appendix D.2, we also present the ECDFs with respect to the runtime for small and large instances in this setting.

As observed in Figure 3, adding valid inequalities results in substantial improvement for all formulations across both small and large instances. While no single formulation dominates in all cases, LBBD consistently

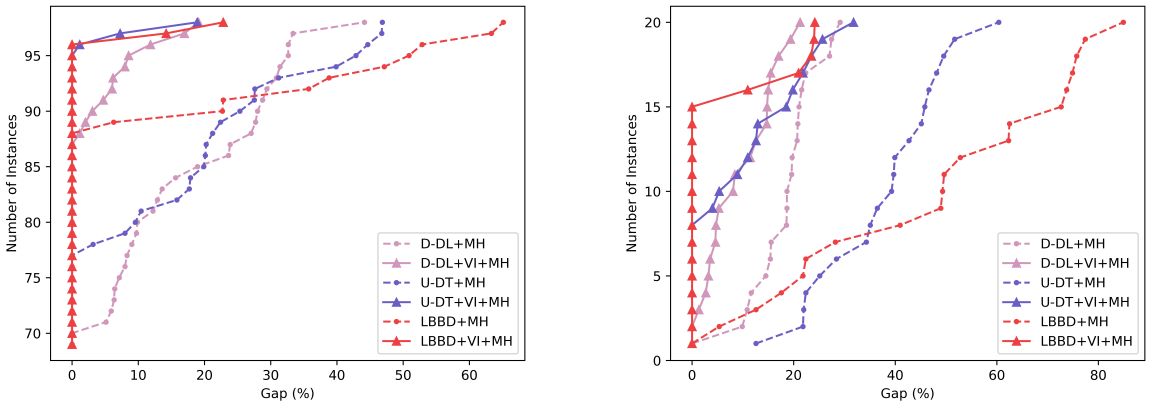

(a) Small Instances

(b) Large Instances

Figure 3: Gap at Termination of Strengthened Formulations with MIP Start Heuristic

solves the most instances to optimality, whereas D-DL shows the best worst-case gap.

In conclusion, the valid inequalities significantly enhance performance for all formulations, with LBBD emerging as the overall best performer.

8 Conclusions

We have addressed the Undirected Team Orienteering Arc Routing Problem and proposed two undirected formulations with binary decision variables: a disaggregated formulation and a semi-aggregated formulation. Based on these formulations, we demonstrated how to decompose this problem using LBBD and strengthen the Benders cuts. Additionally, we derived valid inequalities to further enhance these formulations, which include inaccessible first and second traversal inequalities, clique and IS inequalities (derived from conflict graphs), symmetry breaking constraints, as well as SLBBCs. Based on these formulations, the B&C algorithms are implemented. They are supported by several heuristics to find and improve feasible solutions, alongside efficient procedures for separating and generating valid inequalities. We conducted extensive computational tests to evaluate the performance of the proposed formulations and examined the effects of the MIP start heuristic and valid inequalities. A sensitivity analysis was also implemented to compare the performance of the LBBD formulation with the benchmark formulation D-DL under varying numbers of vehicles and travel time limits.

The computational results highlight the intrinsic difficulty of the considered problem, especially for large instances, where all basic formulations struggle, resulting in numerous unsolved cases and substantial optimality gaps. However, the integration of the MIP start heuristic and, more importantly, the incorporation of valid inequalities led to a significant improvement in performance. Among the tested formulations, as well as the benchmark D-DL, the LBBD formulation—when complemented by the MIP start heuristic and reinforced with valid inequalities—consistently outperformed the others. This advantage was further confirmed through computational experiments across different numbers of vehicles and varying travel time limits.

Our study highlights the transformative potential of LBBD and conflict graphs in advancing ARP research. For multiple-vehicle ARPs, LBBD naturally breaks the problem into a series of smaller, single-vehicle arc routing subproblems, which are significantly easier to handle due to their reduced size. Meanwhile, conflict graphs provide a powerful framework for capturing key structural properties of undirected ARPs, encoding critical problem constraints and interactions. By leveraging these graph structures, the derived valid inequalities effectively strengthen formulations and enhance computational efficiency. Our findings underscore these techniques as promising tools for improving solution methodologies in ARPs.

We would like to express our sincere gratitude to [acknowledge individuals, organizations, or institutions]

for their invaluable contributions to this research. We are also grateful to [mention any additional acknowledgements, such as technical assistance, data providers, or colleagues] for their support and assistance throughout the course of this work.

References

E. Amaldi, M. E. Pfetsch, and L. E. Trotter, Jr. On the maximum feasible subsystem problem, IISs and IIS-hypergraphs. *Mathematical Programming*, 95(3):533–554, 2003.

C. Archetti and M. Speranza. *Arc Routing Problems with Profits*. MOS-SIAM Series on Optimization. SIAM, 2015.

C. Archetti, D. Feillet, A. Hertz, and M. G. Speranza. The undirected capacitated arc routing problem with profits. *Computers & Operations Research*, 37(11):1860–1869, 2010.

C. Archetti, M. G. Speranza, Á. Corberán, J. M. Sanchis, and I. Plana. The Team Orienteering Arc Routing Problem. *Transportation Science*, 48(3):442–457, 2014.

C. Archetti, Á. Corberán, I. Plana, J. M. Sanchis, and M. G. Speranza. A matheuristic for the Team Orienteering Arc Routing Problem. *European Journal of Operational Research*, 245(2):392–401, 2015.

J. Aráoz, E. Fernández, and O. Meza. Solving the Prize-collecting Rural Postman Problem. *European Journal of Operational Research*, 196(3):886–896, 2009.

F. Barahona and M. Grötschel. On the cycle polytope of a binary matroid. *Journal of Combinatorial Theory, Series B*, 40:40–62, 1986.

E. Bartolini, J.-F. Cordeau, and G. Laporte. Improved lower bounds and exact algorithm for the capacitated arc routing problem. *Mathematical Programming*, 137(1-2):409–452, 2013. ISSN 0025-5610, 1436-4646.

E. Benavent, Á. Corberán, L. Gouveia, M. C. Mourão, and L. S. Pinto. Profitable mixed capacitated arc routing and related problems. *TOP*, 23(1):244–274, 2015.

C. Bode and S. Irnich. Cut-First Branch-and-Price-Second for the Capacitated Arc-Routing Problem. *Operations Research*, 60(5):1167–1182, 2012.

I. M. Bomze, M. Budinich, P. M. Pardalos, and M. Pelillo. *The Maximum Clique Problem*, pages 1–74. Springer US, Boston, MA, 1999. ISBN 978-1-4757-3023-4.

J. F. Campbell, A. Langevin, and N. Perrier. *Advances in Vehicle Routing for Snow Plowing*, chapter 14, pages 321–350. MOS-SIAM Series on Optimization. SIAM, 2015.

J. F. Campbell, Á. Corberán, I. Plana, and J. M. Sanchis. Drone arc routing problems. *Networks*, 72(4): 543–559, 2018.

N. Christofides. *An Algorithm for the Rural Postman Problem*. PhD thesis, Imperial College London, 1981.

F. Clautiaux and I. Ljubić. Last fifty years of integer linear programming: A focus on recent practical advances. *European Journal of Operational Research*, 2024.

Á. Corberán and G. Laporte, editors. *Arc routing: problems, methods, and applications*. MOS-SIAM Series on Optimization. SIAM, 2015.

A. Corberán, I. Plana, M. Reula, and J. Sanchis. On the distance-constrained close enough arc routing problem. *European Journal of Operational Research*, 291:32–51, 2021.

A. Corberán and J. M. Sanchis. A polyhedral approach to the rural postman problem. *European Journal of Operational Research*, 79(1):95–114, 1994.

G. B. Dantzig. Discrete-Variable Extremum Problems. *Operations Research*, 5(2):266–288, 1957.

F. Della Croce and R. Tadei. A multi-KP modeling for the maximum-clique problem. *European Journal of Operational Research*, 73(3):555–561, 1994.

M. Dror, editor. *Arc Routing*. Springer New York, NY, Boston, MA, 2000.

R. El-Hajj, D.-C. Dang, and A. Moukrim. Solving the team orienteering problem with cutting planes. *Computers & Operations Research*, 74:21–30, 2016.

J. Euchi and H. Chabchoub. Hybrid metaheuristics for the profitable arc tour problem. *Journal of the Operational Research Society*, 62(11):2013–2022, 2011.

D. Feillet, P. Dejax, and M. Gendreau. The Profitable Arc Tour Problem: Solution with a Branch-and-Price Algorithm. *Transportation Science*, 39(4):539–552, 2005.

T. A. Feo and M. G. C. Resende. Greedy Randomized Adaptive Search Procedures. *Journal of Global Optimization*, 6(2):109–133, 1995.

E. Fernández, M. Leitner, I. Ljubić, and M. Ruthmair. Arc routing with electric vehicles: Dynamic charging and speed-dependent energy consumption. *Transportation Science*, 56(5):1219–1237, 2022.

E. Fernández, I. Ljubić, J. Rodríguez-Pereira, and W. Yan. *Undirected Arc Routing Problems*, chapter 9. Research Handbooks in Transport Studies series. Edward Elgar Publishing Ltd, 2025. forthcoming.

G. Ghiani and G. Laporte. *The Undirected Rural Postman Problem*, chapter 5, pages 85–99. MOS-SIAM Series on Optimization. SIAM, 2015.

G. Ghiani, C. Mourão, L. Pinto, and D. Vigo. *Routing in Waste Collection Applications*, chapter 15, pages 351–370. MOS-SIAM Series on Optimization. SIAM, 2015.

J. Gleeson and J. Ryan. Identifying Minimally Infeasible Subsystems of Inequalities. *ORSA Journal on Computing*, 2(1):61–63, 1990.

A. Gunawan, H. C. Lau, and P. Vansteenwegen. Orienteering Problem: A survey of recent variants, solution approaches and applications. *European Journal of Operational Research*, 255(2):315–332, 2016.

D. Gusfield. Very Simple Methods for All Pairs Network Flow Analysis. *SIAM Journal on Computing*, 19 (1):143–155, 1990.

A. Hertz, G. Laporte, and P. Nanchen-Hugo. Improvement procedures for the undirected rural postman problem. *INFORMS Journal on Computing*, 1:53–62, 1999.

J. Hooker. *Logic-Based Benders Decomposition: Theory and Applications*. Synthesis Lectures on Operations Research and Applications. Springer International Publishing, Cham, 2024.

T. C. Huanfa Chen and J. Shawe-Taylor. A balanced route design for min-max multiple-depot rural postman problem (mmmdrpp): a police patrolling case. *International Journal of Geographical Information Science*, 32(1):169–190, 2018.

C. P. Keller. Algorithms to solve the orienteering problem: A comparison. *European Journal of Operational Research*, 41(2):224–231, 1989.

A. C. Leifer and M. B. Rosenwein. Strong linear programming relaxations for the orienteering problem. *European Journal of Operational Research*, 73(3):517–523, 1994.

J. W. Moon and L. Moser. On cliques in graphs. *Israel Journal of Mathematics*, 3(1):23–28, 1965.

C. Orloff. On general routing problems: Comments. *Networks*, 6(3):281–284, 1976.

M. W. Padberg. On the facial structure of set packing polyhedra. *Mathematical Programming*, 5(1):199–215, 1973.

R. Rahmaniani, T. G. Crainic, M. Gendreau, and W. Rei. The Benders decomposition algorithm: A literature review. *European Journal of Operational Research*, 259(3):801–817, 2017.

J. Riera-Ledesma and J. J. Salazar-González. Solving the Team Orienteering Arc Routing Problem with a column generation approach. *European Journal of Operational Research*, 262(1):14–27, 2017.

E. E. Zachariadis and C. T. Kiranoudis. Local search for the undirected capacitated arc routing problem with profits. *European Journal of Operational Research*, 210(2):358–367, 2011.

A Valid Inequalities

A.1 Inaccessible Traversal Inequalities and Edges in Conflict

We demonstrate the minimum travel time used in inaccessible traversal inequalities and the definition of edges in conflict.

Figure 4a illustrates the minimum travel time $l^1_{0e} = d_{0i} + t_e + d_{j0}$ for edge $e = ij$, where the blue edges represent the shortest path between two vertices.

Figure 4b visualizes the possible tours contributing to the minimum travel time $l^2_{0e} = \min\{d_{0i} + 2t_e + d_{i0}, d_{0j} + 2t_e + d_{j0}\}$ for edge $e = ij$. Starting from the depot 0, a vehicle can travel either from vertex i, covering a distance of d_{0i}, or via vertex j, covering a distance of d_{0j}. After that, the vehicle can traverse the edge e twice, and finally, follow the original path (either d_{i0} or d_{j0}) back to the depot.

Figure 4c depicts the possible tours of contributing to the minimum travel time $L_{\min}(e, e') = \min\{d_{0i} + t_e + d_{ji'} + t_{e'} + d_{j'0}, d_{0i} + t_e + d_{jj'} + t_{e'} + d_{i'0}, d_{0j} + t_e + d_{ii'} + t_{e'} + d_{j'0}, d_{0j} + t_e + d_{ij'} + t_{e'} + d_{i'0}\}$ for edges $e = ij$ and $e' = i'j'$. Starting from the depot 0, a vehicle can reach the edge e by arriving at either vertex i or j. After traversing the edge e, it departs from the opposite vertex and proceeds to the edge e', entering through either vertex i' or j'. The vehicle then traverses the edge e' and returns to the depot from opposite vertex of e'.

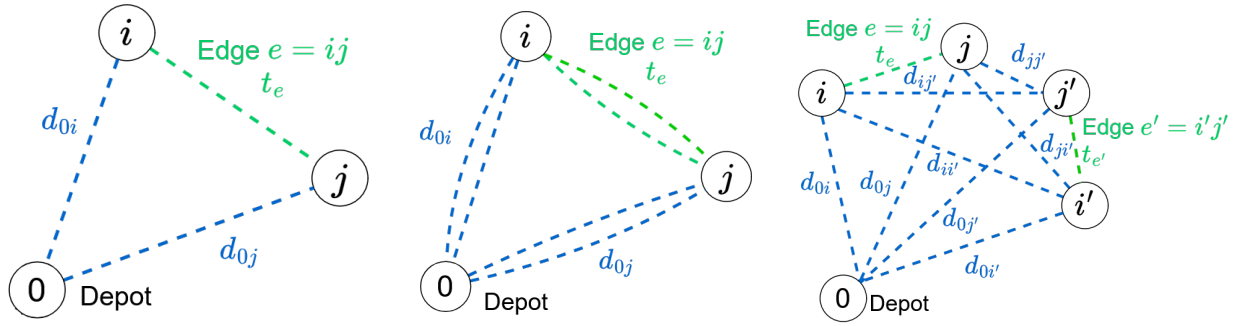

(a) l^1_{0e} (b) l^2_{0e} (c) $L_{\min}(e, e')$

Figure 4: Minimum Travel Time
(a) Tour of Traversing the Edge e Once from the Depot; (b) Tours of Traversing the Edge e Twice from the Depot; (c) Tours of Traversing Two Edges e and e' Once from the Depot

A.2 Symmetry Breaking Constraints for U-ST

The alternative symmetry breaking rules for U-ST are as follows:

(SB4) If a profitable edge e_t is served, then it is traversed at least once by a vehicle with index smaller than or equal to its own index.

(SB5) If a profitable edge e_t is served by vehicle k whose index is larger than t, then vehicle k serves some profitable edge with an index smaller than t (e_q, $q \in \{k, ..., t-1\}$).

They can be written as follows:

$$\text{(SB4)} \qquad z_{e_t} \le \sum_{k=1}^{t} y^k_{e_t}, \qquad \forall e_t \in E_P,\ t \in \{1, ..., |K|\}, \tag{25a}$$

$$\text{(SB5)} \qquad z_{e_t} \le \sum_{k'=1}^{k} y^{k'}_{e_t} + \sum_{q=k}^{t-1} y^k_{e_q}, \qquad \forall e_t \in E_P,\ k = \{1, ..., |K| - 1\},\ k < t. \tag{25b}$$

B Heuristics and Separation Procedures

B.1 Formulation for the URPP induced by a given set of served edges $P(\bar{\mathbf{s}}^k)$ for $k \in K$.

Let $P(\bar{\mathbf{s}}^k)$ be a given a set of profitable edges for vehicle k. We consider as set of required edges $E_R = P(\bar{\mathbf{s}}^k)$ and use the notation $\delta_R(S) = \delta(S) \cap E_R$, where $S \subset V$ is a given subset of vertices. We define the following decision variables:

- $x_e \in \{0,1\}$: is 1 if the edge $e \in E$ is deadheaded for the first time by the vehicle and 0 otherwise;
- $X_e \in \{0,1\}$: is 1 if the edge $e \in E$ is deadheaded for the second time by the vehicle and 0 otherwise.

We recall that, for required edges, deadheads refer to traversals additional to those servicing them. Hence, $X_e = 0$ must hold for all $e \in E_R$.

The URPP formulation is:

$$\sum_{e \in E_R} t_e + \min_{\mathbf{x},\mathbf{X} \in \{0,1\}^{|E|}} \sum_{e \in E} t_e(x_e + X_e) \tag{26a}$$

$$\text{s.t.} \quad (x - X)(\delta(S) \setminus F) + X(F \setminus R) \geq x(F) - |F| + 1, \quad \forall S \subset V,\, F \subseteq \delta(S),\, |F| + |\delta_R(S)| \text{ odd}, \tag{26b}$$

$$(x + X)(\delta(S)) \geq 2, \qquad \forall S \subseteq V \setminus \{0\},\, \delta_R(S) = \emptyset,\, E(S) \cap E_R \neq \emptyset, \tag{26c}$$

$$X_e \leq x_e, \qquad \forall e \in E \setminus E_R, \tag{26d}$$

$$X_e = 0, \qquad \forall e \in E_R. \tag{26e}$$

The objective function (26a) aims to minimize the total travel time of required edges (which is constant) plus deadheaded edges. Co-circuit constraints (26b) guarantee the even degree of each vertex in the vehicle's tour. Given that $|F| + |\delta_R(S)|$ is odd, when $x(F) = |F|$, at least one more edge in $\delta(S)$ must be traversed. Such traversal must be either a second deadhead of an non-required edge of F, or a single deadhead of some edge of $\delta(S) \setminus F$. By constraints (26c), the vehicle's tour is connected. Note that it is enough to only consider vertex sets S with no required edge in their cutsets such that $E(S)$ contains some required edge. Both sets of constraints take into account that all required edges must be traversed. Constraints (26d) impose the condition that an edge cannot be deadheaded for a second time without being deadheaded for the first time, whereas Constraints (26e) state that required edges cannot be deadheaded twice.

As it is usual, we reinforce the LP relaxation of the formulation above with the following inequalities:

$$|\delta_R(S)| + (x + X)(\delta(S)) \geq 2, \qquad \forall S \subseteq V \setminus \{0\},\, E(S) \cap E_R \neq \emptyset, \tag{27}$$

which eliminate violated fractional solutions where the cutset contains required edges.

B.2 Details of Algorithm 1

We now provide a more detailed description of Algorithm 1. For each $k \in K$, the algorithm first applies a path-insertion heuristic to construct a feasible solution $\bar{\psi}^k$ to the URPP with respect to the choice of edges to be served, determined by $H^k = P(\bar{\mathbf{s}}^k)$. Specifically, the process begins with only the depot, $\mathcal{V}_{\bar{H}^k} = \{0\}$, in the vertex set of the tour (i.e., set of served edges $\bar{H}^k = \emptyset$, current travel time $\bar{\tau}^k = 0$, current solution to the URPP $\bar{\psi}^k = \emptyset$). Then, each profitable edge $e \in H^k$ is iteratively inserted into the tour in a greedy order, prioritizing the edge with the minimum travel time $l_e = \min_{i \in \mathcal{V}_{\bar{H}^k}} l^1_{ie}$ (defined in Section 5.1 as the minimum travel time for a vehicle to traverse the edge e once starting and ending at vertex i), relative to the vertices $\mathcal{V}_{\bar{H}^k}$ in the current tour. At each iteration, the unserved edge with the minimum travel time ($e' = i'j' \in \arg\min_{e \in H^k \setminus \bar{H}^k} l_e$) is added to the tour at the vertex that achieves this minimum (i.e., $i_{e'} \in \arg\min_{i \in \mathcal{V}_{\bar{H}^k}} l^1_{ie'}$). The feasible solution $\bar{\psi}^k$ is expanded by including the edge e' along with the associated deadhead edges $L_{i_{e'}e'}$, where $L_{i_{e'}e'}$ represents the set of edges that are deadheaded in order to traverse the edge e' from vertex $i_{e'}$. Specifically, these are the edges of two paths, one connecting $i_{e'}$ to i',

and the other connecting j' to $i_{e'}$. The construction continues until all profitable edges in H^k are included in the tour.

If the travel time of this constructed feasible solution $\bar{\tau}^k$ does not exceed $T_{\max}$, H^k is confirmed as an FPS. Otherwise, the algorithm further evaluates the feasibility of H^k by solving an instance of the URPP, using the previously constructed feasible solution $\bar{\psi}^k$ as an initial feasible solution. If the resulting URPP can serve all the edges from H^k within $T_{\max}$, a feasible tour $\psi^k = (H^k, L^k)$ is stored. Otherwise, the set H^k is an IPS, and in order to insert a violated Benders cut, we proceed by searching for a RIPS. Note that finding a minimum-cardinality infeasible subsystem is an NP-hard problem even for linear programs (Gleeson and Ryan, 1990; Amaldi et al., 2003). We therefore resort to a heuristic approach, which finds a RIPS $\hat{H}^k$, and at the same time, returns a feasible tour $\psi^k = (H^k, L^k)$.

Given an IPS H^k, identifying a RIPS $\hat{H}^k \subset H^k$ involves removing elements from H^k, with each removal requiring the solution to a URPP. We apply a greedy heuristic (see Algorithm 2) which removes the current *closest* edge until the IPS H^k becomes an FPS (see, e.g., Hooker, 2024). For an IPS H^k, the *closest* edge e' is defined as the edge $e \in H^k$ that minimizes the distance l^1_{ie} from any vertex i in V_{H^k} (i.e., $e' \in_{i \in V_{H^k}, e \in H^k} l^1_{ie}$), where V_{H^k} is the set of all end-vertices of edges in H^k (i.e., $V_{H^k} = \{i \in V \mid i \text{ is an end-vertex of } e, \text{for some } e \in H^k\}$). This FPS, together with the set of deadheaded edges L^k is stored as a feasible tour for vehicle k. The FPS, enlarged with the last removed element, forms a RIPS $\hat{H}^k$.

Algorithm 2: Find a RIPS

Input: An IPS H^k, a constructed feasible solution $\bar{\psi}^k$ of the URPP, the time limit $T_{\max}$
Output: A RIPS $\hat{H}^k$, a feasible solution ψ^k of the tour k

function `Find_a_RIPS`$(H^k, \bar{\psi}^k, T_{\max})$
  $V_{H^k} \leftarrow \{i \in V | i \text{ is an end-vertex of } e, e \in H^k\}$;
  repeat
    Choose the closest edge $e' \in_{i \in V_{H^k}, e \in H^k} l^1_{ie}$;
    Set $H^k \leftarrow H^k \setminus \{e'\}$, $V_{H^k} \leftarrow \{i \in V | i \text{ is an end-vertex of } e, e \in H^k\}$;
    Solve an instance of the URPP of H^k with $\bar{\psi}^k$ as an initial feasible solution. Let $T^*(H^k)$ be the returned objective value and $\psi^k = (H^k, L^k)$ the returned feasible solution;
  until $T^*(H^k) \leq T_{\max}$;
  Set $\hat{H}^k \leftarrow H^k \cup \{e'\}$;
  Return $\hat{H}^k$, ψ^k.

In the last phase of the algorithm, we apply the *Improvement Heuristic*, which aims to enhance the tour (H^k, L^k) by serving additional profitable edges that are deadheaded in the current tour but not served in any other tour. Specifically, for each edge e that is not served by any vehicle k (i.e., $e \in E_P \setminus \mathcal{H}$), if it is deadheaded in the current tour representing the feasible URPP solution for vehicle k (i.e., $e \in L^k$), edge e is included into H^k and the set $\mathcal{H}$ is updated correspondingly.

B.3 Formulations for the MCP and MWCP

Formulations from Edge Conflict Graph G_c for U-DT and U-ST For the MCP, the formulation is adapted from the edge formulation (see, e.g., Bomze et al., 1999). Let θ_e be the binary decision variable that indicates whether or not the edge e is chosen in the clique. Assume the profitable edge with the highest profit that has not been included in any clique is e', then we solve the following MCP based on the edge conflict graph G_c:

$$\max_{\theta \in \{0,1\}^{E \setminus E^1}} \quad \sum_{E \setminus E_1} \theta_e \tag{28a}$$

$$\text{s.t.} \quad \theta_e + \theta_f \leq 1, \quad \forall e, f \in E \setminus E^1,\ L_{\min}(e, f) \leq T_{\max}, \tag{28b}$$

$$\theta_{e'} = 1. \tag{28c}$$

The objective function (28a) is to maximize the total number of edges in the clique. Constraints (28b) require that if two edges e and f are not in conflict, only one edge can be included in the clique. With constraints (28c), the edge e' must be included in the clique.

For the MWCP, weights are assigned to edges based on their profitability. Specifically, we define the weight of each profitable edge $e \in E_P \setminus E_P^1$ as $r_e + 1$ and the weight of each non-profitable edge $e \in E_{NP} \setminus E_{NP}^1$ as 1. The MWCP replaces the objective function (28a) with the following:

$$\max_{\theta \in \{0,1\}^{E \setminus E^1}} \quad \sum_{e \in E_P \setminus E_P^1} (r_e + 1)\theta_e + \sum_{e \in E_{NP} \setminus E_{NP}^1} \theta_e. \tag{29}$$

The constraints remain the same as in (28b) - (28c).

Formulations from Edge Conflict Graph $G_c[E_P]$ for LBBD Since $G_c[E_P]$ is a subgraph of G_c, the formulations for the MCP and MWCP from G_c can be directly applied to $G_c[E_P]$, limiting the domain of the decision variables to profitable edges $E_P \setminus E_P^1$.

B.4 MIP Start Heuristic

The pseudocode is presented in Algorithm 3.

Algorithm 3: MIP Start Heuristic

Input: the travel time limit $T_{\max}$, fraction of candidates γ for the candidate list
Output: a feasible solution ψ

$\mathcal{H} \leftarrow \emptyset$;
for $k \in K$ **do**
  $\tau^k \leftarrow 0$, $H^k \leftarrow \emptyset$, $\mathcal{V}_{H^k} \leftarrow \{0\}$, $\bar{\psi}^k \leftarrow \emptyset$;
  repeat
    $SolutionChange \leftarrow False$;
    repeat `// Search for a candidate`
      $\mathcal{W} \leftarrow \{w_e \mid e \in E_P \setminus \mathcal{H}\}$ where $w_e = \max_{i \in V_{H^k}} \{\frac{r_e}{l^1_{ie}} | \tau^k + l^1_{ie} \le T_{\max}\}$, and let $i_e \in \arg\max_{i \in V_{H^k}} \{\frac{r_e}{l^1_{ie}} | \tau^k + l^1_{ie} \le T_{\max}\}$;
      if $\mathcal{W} \neq \emptyset$ **then** `// Select a candidate`
        Sort edges from $E_P \setminus \mathcal{H}$ in non-increasing order according to $w \in \mathcal{W}$;
        Randomly choose one $e' = i'j'$ from the top γ fraction of the sequence of $E_P \setminus \mathcal{H}$;
        Update $\mathcal{H} \leftarrow \mathcal{H} \cup \{e'\}$, $H^k \leftarrow H^k \cup \{e'\}$, $\tau^k \leftarrow \tau^k + l^1_{i_{e'}e'}$, $\mathcal{V}_{H^k} \leftarrow \mathcal{V}_{H^k} \cup \{i'\} \cup \{j'\}$, $\bar{\psi}^k \leftarrow \bar{\psi}^k \cup (e', L_{i_{e'}e'})$;
        $SolutionChange \leftarrow True$;
    until $\mathcal{W} = \emptyset$;
    if $SolutionChange \leftarrow True$ **then**
      Solve a URPP of H^k with $\bar{\psi}^k$ as initial solultion, and let $\psi^k = (H^k, L^k)$ be a feasible solution obtained from the URPP and $T^*(H^k)$ the corresponding objective value;
      $\tau^k \leftarrow T^*(H^k)$;
      for $e \in E_P \setminus \mathcal{H}$ **do** `// Improvement Heuristic`
        if $e \in L^k$ **then** $H^k \leftarrow H^k \cup \{e\}$, $L^k \leftarrow L^k \setminus \{e\}$, $\psi^k \leftarrow (H^k, L^k)$, $\mathcal{H} \leftarrow \mathcal{H} \cup \{e\}$, $\mathcal{V}_{H^k} \leftarrow \mathcal{V}_{H^k} \cup \{i\} \cup \{j\}$, where $e = ij$;
  until $SolutionChange = False$;
  $\psi = \psi \cup \{\psi^k\}$;
Return the feasible UTOARP solution ψ.

To better explain the pseudocode, we need more notation. Let τ^k be the travel time of the current tour $k \in K$. Let w_e be the maximum weight defined by the profit r_e of unserved edge $e \in E_P \setminus \mathcal{H}$ divided by

the minimum travel time l^1_{ie} over all vertices $i \in V_{H^k}$, provided that the edge e can be served within the travel time limit based on the current tour's travel time, i.e., $w_e = \max_{i \in V_{H^k}} \{\frac{r_e}{l^1_{ie}} | \tau^k + l^1_{ie} \leq T_{\max}\}$. Let $\mathcal{W}$ be the set of candidate weights w_e for unserved edge $e \in E_P \setminus \mathcal{H}$. Let i_e be the corresponding vertex in V_{H^k} that achieves the maximum feasible weight $\frac{r_e}{l^1_{ie}}$ of edge e, i.e., $i_e \in \arg\max_{i \in V_{H^k}} \{\frac{r_e}{l^1_{ie}} | \tau^k + l^1_{ie} \leq T_{\max}\}$. Let $\bar{\psi}^k = (H^k, \bar{L}^k)$ be a trivial feasible solution for the URPP of H^k, constructed from the subtour (e, L_{ie}), where edge e is served from vertex i and L_{ie} is the set of edges deadheaded to serve edge e from vertex i. Let γ be the fraction of candidates kept in the candidate set, which is set to 0.25 in our tests. Finally, let c_{count} count the number of candidates selected and c_{last} stores the number of candidates before solving a URPP.

For each tour $k \in K$, we initialize the vertex set V_{H^k} with only the depot and choose the candidates from all unserved profitable edges $e \in E_P \setminus \mathcal{H}$. For each such edge e, we calculate the weight w_e as defined above, and add it to the candidate set $\mathcal{W}$ and record the corresponding vertex i_e. We then randomly choose the next profitable edge $e' \in E_P \setminus \mathcal{H}$ to visit from the candidate set $\mathcal{W}$ based on the fraction γ, and update all related sets $\mathcal{H}$, H^k, τ^k, V_{H^k}. A feasible solution $\bar{\psi}^k$ of tour k is constructed by inserting the chosen profitable edge e' into the tour at vertex $i_{e'}$, along with the deadhead edges $L_{i_{e'}e'}$ (i.e., $\bar{\psi}^k = \bar{\psi}^k \cup (e', L_{i_{e'}e'})$). We repeat this procedure until no candidate is found. We then solve a URPP for H^k with $\bar{\psi}^k$ as an initial feasible solution, which enables us to find the minimum travel time $T^*(H^k)$, and hence gives us the chance to continue the previous search procedure. The feasible solution found by the URPP will be improved by seeking edges traversed in the current tour but not served by any other vehicle. The algorithm stops when no candidate is found after solving the URPP.

C Compact Load-based Formulation on the Bidirected Graph

C.1 Notation

The *compact formulation* we present for the UTOARP is derived from a bidirected counterpart of the original undirected graph G, where each edge $e = ij \in E$ is substituted by two arcs $a^+ = (i, j)$ and $a^- = (j, i)$ with opposite directions, assigning the corresponding profit r_e and travel time t_e to each arc. The bidirected counterpart of G will be denoted as $\overline{G} = (V, A)$, where the set of arcs $A = A_P \cup A_{NP}$ with A_P and A_{NP} being the set of profitable arcs and non-profitable arcs, respectively. For a node $i \in V$, let $\delta^+(i) = \{a = (i, j) \in A \mid j \in V \setminus \{i\}\}$ be the set of arcs leaving i and $\delta^-(i) = \{a = (j, i) \in A \mid j \in V \setminus \{i\}\}$ be the set of arcs entering i. Additionally, for a node $i \in V$, let $\delta^+_P(i) = \delta^+(i) \cap A_P$ as the set of profitable arcs leaving S and $\delta^-_P(i) = \delta^-(i) \cap A_P$ as the set of profitable arcs entering S. For simplicity, the summation of a vector $y \in \mathbb{R}^{|A|}$ over a set $F \subset A$ is written as $y(F) = \sum_{a \in F} y_a$.

C.2 Formulation

A compact load-based formulation on the bidirected graph $\overline{G}$ is an adaptation of the formulation of Benavent et al. (2015), which was initially proposed for the TOARP on *mixed* graphs. This formulation is valid only if each vehicle $k \in K$ leaves and enters the depot $0 \in V$ just once. To accommodate this condition, we can add an artificial depot $0'$ to the node set V, connecting it to the original depot 0 with two zero-cost arcs in opposite directions.

On the bidirected graph, the optimality condition (cf. Section 2.2) implies that an optimal solution exists, where each arc is traversed at most once by each vehicle. Therefore, we can model the problem using binary variables for deadhead of each arc. This is the main difference compared to the model for mixed graphs by Benavent et al. (2015), where the number of deadheads can be larger than one, and therefore integer deadhead variables must be used instead. In our case, we use the following variables:

- $s^k_{ij} \in \{0, 1\}$: indicates if profitable arc $(i, j) \in A_P$ is served by vehicle $k \in K$;
- $x^k_{ij} \in \{0, 1\}$: indicates if arc $(i, j) \in A$ is deadheaded by vehicle $k \in K$;
- $f^k_{ij} \geq 0$: represents the load (travel time) on arc $(i, j) \in A$ for vehicle $k \in K$.

The formulation on the bidirected graph (which we will denote by D-DL) is given by:

$$\max_{\substack{\mathbf{s}\in\{0,1\}^{|A_P||K|}\\ \mathbf{y}\in\{0,1\}^{|A||K|}\\ \mathbf{f}\in\mathbb{R}^{|A||K|}}} \sum_{k\in K}\sum_{(i,j)\in A_P} r_{ij}s^k_{ij} \tag{30a}$$

$$\text{s.t.} \sum_{k\in K}(s^k_{ij}+s^k_{ji}) \le 1, \qquad \forall e=ij\in E_P, \tag{30b}$$

$$s^k(\delta^+_P(i)) + x^k(\delta^+(i)) = s^k(\delta^-_P(i)) + x^k(\delta^-(i)), \qquad \forall i\in V,\, k\in K, \tag{30c}$$

$$f^k(\delta^-(i)) - f^k(\delta^+(i)) = \sum_{(j,i)\in\delta^-_P(i)} t_{ji}s^k_{ji} + \sum_{(j,i)\in\delta^-(i)} t_{ji}x^k_{ji}, \qquad \forall i\in V\setminus\{0'\},\, k\in K, \tag{30d}$$

$$f^k(\delta^+(0')) = \sum_{(i,j)\in A_P} t_{ij}s^k_{ij} + \sum_{(i,j)\in A} t_{ij}x^k_{ij}, \qquad \forall k\in K, \tag{30e}$$

$$f^k(\delta^-(0')) = 0, \qquad \forall k\in K, \tag{30f}$$

$$0 \le f^k_{ij} \le T_{\max}(s^k_{ij}+x^k_{ij}), \qquad \forall (i,j)\in A_P,\, k\in K, \tag{30g}$$

$$0 \le f^k_{ij} \le T_{\max}x^k_{ij}, \qquad \forall (i,j)\in A_{NP},\, k\in K, \tag{30h}$$

$$s^k_{ij}+x^k_{ij} \le 1, \qquad \forall (i,j)\in A_P,\, k\in K. \tag{30i}$$

The objective function (30a) is to maximize the total profits collected over all the vehicles. Constraints (30b) guarantee that each profitable edge is served at most once across all vehicles. Equations (30c) maintain the parity of each node in the tour of each vehicle. Equations (30d) balance, for each vehicle, the load at nodes other than the artificial depot, enforcing that the load entering a given node minus the load leaving it equals the total travel time of the entering arcs. Equations (30e) set the load of each vehicle leaving the artificial depot equal to the total travel time of its tour, while equations (30f) ensure the load of each vehicle entering the artificial depot is zero. Constraints (30g) and (30h) impose upper bounds on the load of each profitable and non-profitable arc for each vehicle, respectively, ensuring the travel time limit $T_{\max}$ is respected. Constraints (30i) prevent a profitable arc from being served and deadheaded simultaneously by the same vehicle.

Formulation D-DL is compact but involves $2(|E|+|E_P|)|K|$ binary variables, potentially resulting in a large B&B tree.

C.3 Valid Inequalities

The above mentioned valid inequalities in Section 5 can be adapted to D-DL as follows:

C.3.1 Inequalities for Inaccessible Traversals

For inaccessible first traversals, we forbid service and deadhead of arcs in both directions:

$$\sum_{e=ij\in E^1_P,k\in K}(s^k_{ij}+s^k_{ji}+x^k_{ij}+x^k_{ji}) = 0, \tag{31a}$$

$$\sum_{e=ij\in E^1_{NP},k\in K}(x^k_{ij}+x^k_{ji}) = 0. \tag{31b}$$

For inaccessible second traversals, we limit service and deadhead of arcs in both directions to at most once:

$$s^k_{ij}+s^k_{ji}+x^k_{ij}+x^k_{ji} \le 1, \qquad \forall e=ij\in E^2_P,\, k\in K, \tag{32a}$$

$$x^k_{ij}+x^k_{ji} \le 1, \qquad \forall e=ij\in E^2_{NP},\, k\in K. \tag{32b}$$

C.3.2 Inequalities from Conflict Graphs

Since the objective function contains only service variables $\mathbf{s}$, we prioritize inequalities involving service variables $\mathbf{s}$ and incorporate as many deadhead variables $\mathbf{x}$ as possible.

Clique Inequalities from Edge Conflict Graph G_c

Proposition C.1. *Given an MCC $\mathcal{U}$ in G_c, for each clique $U \in \mathcal{U}$, the following clique inequalities are valid for D-DL:*

$$\sum_{e=ij \in U \cap E_P} (s_{ij}^k + s_{ji}^k) + \sum_{e=ij \in U \cap E^2} (x_{ij}^k + x_{ji}^k) + \sum_{e=ij \in U \cap (E_{NP} \setminus E_{NP}^2)} (x_{ij}^k \text{ or } x_{ji}^k) \leq 1, \quad \forall U \in \mathcal{U},\, k \in K. \quad (33)$$

The number of such inequalities is $2^{|U \cap (E_{NP} \setminus E_{NP}^2)|}$ for each $U \in \mathcal{U}$.

Proof. To validate the inequalities, it suffices to show that the extended set $U^{sx} = \{s_{a^+}, s_{a^-} \mid e \in U \cap E_P\} \cup \{x_{a^+}, x_{a^-} \mid e \in U \cap E^2\} \cup \{x_{a^+} \text{ or } x_{a^-} \mid e \in U \cap (E_{NP} \setminus E_{NP}^2)\}$ forms a clique. Indeed, any two variables in U^{sx} are in conflict due to either the conflict relationships among edges in G_c or constraints (30b) and (32). □ □

To create a more compact representation of the inequalities (33), we take their sum and normalize by $2^{|U \cap (E_{NP} \setminus E_{NP}^2)|}$ for each clique $U \in \mathcal{U}$:

Corollary C.2. *Given an MCC $\mathcal{U}$ in G_c, for each clique $U \in \mathcal{U}$, the following clique inequalities are valid for D-DL:*

$$\sum_{e=ij \in U \cap E_P} (s_{ij}^k + s_{ji}^k) + \sum_{e \in U \cap E^2} (x_{ij}^k + x_{ji}^k) + \sum_{e=ij \in U \cap (E_{NP} \setminus E_{NP}^2)} (\frac{1}{2} x_{ij}^k + \frac{1}{2} x_{ji}^k) \leq 1, \quad \forall U \in \mathcal{U},\, k \in K. \quad (34)$$

Proof. Trivial. □ □

Independent Set Inequalities from Variable Conflict Graph For the compact formulation D-DL, the variable conflict graph G_c^{DDL} is constructed with $\mathbf{s}$ and $\mathbf{x}$ variables for each pair of arcs a^+ and a^-, forming the vertex set V_c^{DDL}. Each pair of distinct variables in $V_c^{DDL}$is connected by an edge if at most one of them can take the value one, thereby composing the edge set E_c^{DDL}. Furthermore,

- The linking constraints (30i) impose an edge in G_c^{DDL} between s_{a^+} and x_{a^+}, s_{a^-} and x_{a^-} for each profitable edge $e = (a^+, a^-) \in E_P \setminus E_P^1$.
- The service constraints (30b) impose an edge between s_{a^+} and s_{a^-} for each profitable edge $e = (a^+, a^-) \in E_P \setminus E_P^1$.
- The constraints for inaccessible second traversals (32a) and (32b) impose edges between s_{a^+} and s_{a^-}, s_{a^+} and x_{a^+}, s_{a^+} and x_{a^-}, s_{a^-} and x_{a^+}, s_{a^-} and x_{a^-}, and, x_{a^+} and x_{a^-}, respectively, for each profitable edge $e = (a^+, a^-) \in E_P^2$, and between x_{a^+} and x_{a^-} for each non-profitable edge $e = (a^+, a^-) \in E_{NP}^2$.

The formal definition is:

Definition 6. *A conflict graph of variables for D-DL is $G_c^{DDL} = (V_c^{DDL}, E_c^{DDL})$, where*

$$\begin{aligned}
V_c^{DDL} =& \{s_{a^+}, s_{a^-} \mid e = (a^+, a^-) \in E_P \setminus E_P^1\} \cup \{x_{a^+}, x_{a^-} \mid e = (a^+, a^-) \in E \setminus E^1\} \\
E_c^{DDL} =& \{uv | u, v \in V_c^{DDL},\, u \neq v,\, L_{\min}(edge(u), edge(v)) > T_{\max}\} \\
& \cup \{s_{a^+}x_{a^+},\, s_{a^-}x_{a^-},\, s_{a^+}s_{a^-} \mid e = (a^+, a^-) \in E_P \setminus E_P^1\} \\
& \cup \{s_{a^+}s_{a^-},\, s_{a^+}x_{a^+},\, s_{a^+}x_{a^-},\, s_{a^-}x_{a^+},\, s_{a^-}x_{a^-} \mid e = (a^+, a^-) \in E_P^2\} \\
& \cup \{x_{a^+}x_{a^-} \mid e = (a^+, a^-) \in E^2\}
\end{aligned}$$

where $edge(u)$ maps the arc associated with the variables u from the bidirected graph $\overline{G}$ into the corresponding edge in the undirected graph G.

For D-DL, the IS inequalities are imposed for each service variables $\mathbf{s}$ in G_c^{DDL}, as follows:

Proposition C.3. *For each s_{ij}, $e = ij \in E_P$ in G_c^{DDL}, let α_e^V be the size of the maximum independent set in the subgraph of G_c^{DDL} induced by s_{ij} and its neighbors, and N_e be the set of edges in conflict with e, the IS inequalities for s_{ij} below are valid for D-DL:*

$$\alpha_e^V s_{ij}^k + s_{ji}^k + x_{ij}^k + \sum_{e'=i'j' \in N_e \cap E_P} (s_{i'j'}^k + s_{j'i'}^k) + \sum_{e'=i'j' \in N_e} (x_{i'j'}^k + x_{j'i'}^k) \leq \alpha_e^V, \qquad \forall e = ij \in E_P \setminus E_P^2,\, k \in K, \tag{35a}$$

$$\alpha_e^V (s_{ij}^k + s_{ji}^k + x_{ij}^k + x_{ji}^k) + \sum_{e'=i'j' \in N_e \cap E_P} (s_{i'j'}^k + s_{j'i'}^k) + \sum_{e'=i'j' \in N_e} (x_{i'j'}^k + x_{j'i'}^k) \leq \alpha_e^V, \quad \forall e = ij \in E_P^2,\, k \in K. \tag{35b}$$

Proof. Trivial. See proof of proposition 5.7. □ □

C.3.3 Symmetry Breaking Constraints

For D-DL, based on (23a)-(23c), each edge e_t should be replaced by the corresponding pair of arcs e_t^+ and e_t^-:

$$\text{(SB1)} \quad s_{e_t^+}^k + s_{e_t^-}^k = 0, \qquad \forall e_t \in E_P,\, t \in \{1, ..., |K|-1\},\, k \in \{t+1, ..., |K|\}, \tag{36a}$$

$$\text{(SB2)} \quad s_{e_t^+}^k + s_{e_t^-}^k \leq \sum_{q=k-1}^{t-1} (s_{e_q^+}^{k-1} + s_{e_q^-}^{k-1}), \quad \forall k \in \{2, ..., |K|\},\, t = \{k, ..., |E_P|\}, \tag{36b}$$

$$\text{(SB3)} \quad x_{ij}^k \leq \sum_{k'=1}^{k} (s_{ij}^{k'} + s_{ji}^{k'}), \qquad \forall e = ij \in E_P,\, k \in K, \tag{36c}$$

$$x_{ji}^k \leq \sum_{k'=1}^{k} (s_{ij}^{k'} + s_{ji}^{k'}), \qquad \forall e = ij \in E_P,\, k \in K. \tag{36d}$$

C.3.4 Strengthened Logic-Based Benders Cuts

For D-DL, the SLBBCs can be lifted with constraints (32a):

$$\sum_{e=ij \in H \setminus E_P^2} (s_{ij}^k + s_{ji}^k) + \sum_{e=ij \in H \cap E_P^2} (s_{ij}^k + s_{ji}^k + x_{ij}^k + x_{ji}^k) \leq |H| - 1, \quad \forall k \in K,\, H \subseteq E_P \text{ irreducible IPS}. \tag{37}$$

D Computational Results

D.1 Benchmark Instances

The benchmark instances, originally proposed as the benchmark instances for the URPP (see `https://www.uv.es/plani/instancias.html`), are of varying sizes and characteristics, which can be identified by the first letter of their labels. Instances labeled "P" are the 20 random graphs of Christofides (1981). Instances labeled "D", 'G", and "R" were generated by Hertz et al. (1999). In each of these groups there are nine instances for each number of vertices $n \in \{16, 36, 64, 100\}$. Instances labeled with "D" correspond to graphs with vertices of degree four and disconnected required edge sets; instances labeled "G" are grids with disconnected required edge sets; and instances labeled "R" are random graphs. ALBAIDAA and ALBAIDAB were obtained from the road map of the city of Albaida in Spain (see Corberán and Sanchis (1994) for details).

Table 7 summarizes the details: for each group (column Group), we list the name of the instance set (column Instance Set), the number of instances in the set (column #Instances), the number of vertices (column $|V|$), edges (column $|E|$), and profitable edges (column $|E_P|$), as well as the total profits (column Profit).

Group	Instance set	#Instances	$\|V\|$	$\|E\|$	$\|E_P\|$	Profit
Small	D16	9	16	31-32	3-16	239-1276
	D36	9	36	72	10-38	429-2554
	D64	9	64	128	27-75	1360-3751
	G16	9	16	24	3-13	6-26
	G36	9	36	60	11-35	23-71
	G64	9	64	112	24-68	51-140
	P	24	7-50	10-184	4-78	27-1016
	R20	5	20	37-75	3-7	12664-40945
	R30	5	30	70-111	7-11	23193-48140
	R40	5	40	82-203	8-18	25558-79685
	R50	5	50	130-203	13-20	32412-70925
Large	D100	9	100	200	50-121	1741-4431
	G100	9	100	180	41-113	85-228
	ALBAIDAA	1	102	160	99	15211
	ALBAIDAB	1	90	144	88	11535

Table 7: Summary of Instances

D.2 ECDFs for Runtime

The ECDFs for runtime are depicted in Figure 5. From this figure, the improvements brought by valid inequalities are clear for all formulations. LBBD performs best in both small and large instances. D-DL, however, is dominated by the other formulations in terms of runtime for both instance sizes.

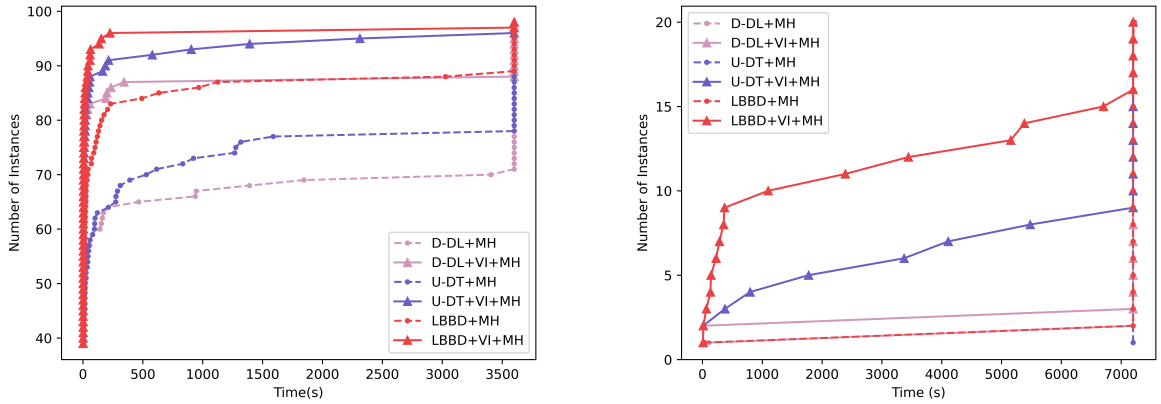

(a) Small instances

(b) Large instances

Figure 5: Runtime of Strengthened Formulations with MIP Start Heuristic

D.3 Sensitivity Analysis

In this group of tests, we investigate the performance of LBBD (as our most robust and best performing approach) under different values for the travel time limit $T_{\max}$ (by varying $\beta \in \{0.6, 0.8, 1.0\}$) and for the number of vehicles $|K| \in \{3, 4, 5\}$. The directed formulation D-DL serves as the benchmark, and both formulations are enhanced with valid inequalities and the MIP start heuristic, as described in Section 7.4. The results are summarized in Tables 8 and 9.

For small instances in Table 8, LBBD consistently outperforms D-DL in terms of the number of instances solved to optimality, average number of branching nodes, and average runtime. However, for the average optimality gap, D-DL performs slightly better in two cases where $\beta = 0.6$, with a gap difference of less than 2%. For large instances in Table 9, LBBD continues to outperform D-DL in the number of instances

β	$\|K\|$	Setting (+VI+MH)	#Optimality	Set (a)			Set (b)	
				#Instances	Time (s)	Nodes	#Instances	Gap (%)
0.6	3	LBBD	**96/98**	89/98	**4.27**	**43**	9/98	**5.13%**
		D-DL	89/98		95.73	19103		7.42%
	4	LBBD	**97/98**	93/98	**3.63**	**3**	5/98	8.02%
		D-DL	93/98		55.81	4377		**5.33%**
	5	LBBD	97/98	97/98	**2.85**	**0**	1/98	24.38%
		D-DL	97/98		4.89	28		**21.68%**
0.8	3	LBBD	**94/98**	84/98	**14.24**	**481**	14/98	**5.97%**
		D-DL	84/98		99.50	9648		8.78%
	4	LBBD	**96/98**	87/98	**4.18**	**13**	11/98	**3.37%**
		D-DL	87/98		15.96	2145		7.96%
	5	LBBD	**97/98**	94/98	**4.03**	**2**	4/98	**7.65%**
		D-DL	94/98		30.61	2022		9.15%
1.0	3	LBBD	**89/98**	80/98	**24.00**	**5618**	18/98	**5.51%**
		D-DL	80/98		170.60	18447		7.08%
	4	LBBD	**95/98**	84/98	**5.17**	**4**	14/98	**3.81%**
		D-DL	84/98		37.19	6687		9.02%
	5	LBBD	**96/98**	87/98	**4.22**	**1**	11/98	**1.84%**
		D-DL	87/98		28.57	2662		8.23%

Table 8: Performance of LBBD and D-DL under Different Values of β and $|K|$ for Small Instances

β	$\|K\|$	Setting (+VI+MH)	#Optimality	Set (a)			Set (b)	
				#Instances	Time (s)	Nodes	#Instances	Gap (%)
0.6	3	LBBD	**15/20**	5/20	**46.29**	**2748**	15/20	**5.24%**
		D-DL	5/20		1339.93	146925		11.17%
	4	LBBD	**20/20**	10/20	**21.22**	**378**	10/20	**0.00%**
		D-DL	10/20		424.92	11087		8.56%
	5	LBBD	**20/20**	16/20	**12.99**	**9**	4/20	**0.00%**
		D-DL	16/20		85.20	7059		8.15%
0.8	3	LBBD	**4/20**	2/20	**14.95**	**10**	18/20	17.81%
		D-DL	2/20		49.69	15735		**9.05%**
	4	LBBD	**15/20**	2/20	12.33	0	18/20	**5.75%**
		D-DL	2/20		**11.40**	0		10.20%
	5	LBBD	**19/20**	9/20	**26.91**	**1**	11/20	**0.66%**
		D-DL	9/20		355.51	43132		10.03%
1.0	3	LBBD	8/20	8/20	**741.68**	**307**	12/20	30.78%
		D-DL	8/20		2127.33	281242		**12.76%**
	4	LBBD	**7/20**	5/20	**397.83**	0	15/20	12.72%
		D-DL	5/20		399.57	0		**12.39%**
	5	LBBD	**14/20**	3/20	**123.78**	**3**	17/20	**4.11%**
		D-DL	3/20		262.79	7000		8.57%

Table 9: Performance of LBBD and D-DL under Different Values of β and $|K|$ for Large Instances

solved to optimality. In most cases, LBBD also achieves lower average runtime, fewer branching nodes, and a smaller average gap. However, D-DL occasionally performs better in certain cases, with gap differences reaching up to 18%. This discrepancy can be attributed to the compact nature of D-DL, which allows the solver to exploit full problem information from the outset, leading to stronger lower and upper bounds. In contrast, LBBD, being a decomposition-based approach, relies on a B&C procedure, which incrementally refines the bounds and may result in weaker bounds in some instances.